

Synthesis of zinc sulfide nanoparticles using microemulsion
generated by hydrodynamic cavitation method



A Thesis Submitted in Partial Fulfillment of the Requirements
for the Degree of Master of Engineering in Chemical Engineering
Department of Chemical Engineering
FACULTY OF ENGINEERING
Chulalongkorn University
Academic Year 2021
Copyright of Chulalongkorn University

การสังเคราะห์อนุภาคซิงค์ซัลไฟด์ระดับนาโนเมตรโดยใช้ไมโครอิมัลชันที่สร้างด้วยวิธีไฮโดรโค
นามิกควิเทชัน



วิทยานิพนธ์นี้เป็นส่วนหนึ่งของการศึกษาตามหลักสูตรปริญญาวิศวกรรมศาสตรมหาบัณฑิต
สาขาวิชาวิศวกรรมเคมี ภาควิชาวิศวกรรมเคมี
คณะวิศวกรรมศาสตร์ จุฬาลงกรณ์มหาวิทยาลัย
ปีการศึกษา 2564
ลิขสิทธิ์ของจุฬาลงกรณ์มหาวิทยาลัย

Thesis Title	Synthesis of zinc sulfide nanoparticles using microemulsion generated by hydrodynamic cavitation method
By	Miss Nachapa Choojan
Field of Study	Chemical Engineering
Thesis Advisor	Professor TAWATCHAI CHARINPANITKUL, D.Eng.
Thesis Co Advisor	Dr. CHARUSLUK VIPHAVAKIT, Ph.D.

Accepted by the FACULTY OF ENGINEERING, Chulalongkorn University
in Partial Fulfillment of the Requirement for the Master of Engineering

..... Dean of the FACULTY OF
ENGINEERING
(Professor SUPOT TEACHAVORASINSKUN, D.Eng.)

THESIS COMMITTEE

..... Chairman
(Assistant Professor APINAN SOOTTITANTAWAT,
D.Eng.)

..... Thesis Advisor
(Professor TAWATCHAI CHARINPANITKUL,
D.Eng.)

..... Thesis Co-Advisor
(Dr. CHARUSLUK VIPHAVAKIT, Ph.D.)

..... Examiner
(Assistant Professor Rungthiwa Methaapanon, Ph.D.)

..... External Examiner
(Assistant Professor Prakorn Kittipoomwong, Ph.D.)

จุฬาลงกรณ์มหาวิทยาลัย
CHULALONGKORN UNIVERSITY

ฉกษา ชูจันทร์ : การสังเคราะห์อนุภาคซิงค์ซัลไฟด์ระดับนาโนเมตร โดยใช้ไมโครอิมัลชันที่สร้างด้วยวิธีไฮโดรไดนามิกคาวิเทชัน. (Synthesis of zinc sulfide nanoparticles using microemulsion generated by hydrodynamic cavitation method) อ.ที่ปรึกษาหลัก : ศ. ดร.รวิชัย ชรินพานิชกุล, อ.ที่ปรึกษาร่วม : ดร.จรัสรัถ วิกาวกิจ

อนุภาคนาโนสังกะสีซัลไฟด์ (ZnS) ได้รับความสนใจในการศึกษาวิจัยเป็นอย่างมากในปัจจุบัน เพื่อนำมาผลิตเป็น สารกึ่งตัวนำ โดยขนาดอนุภาคเป็นปัจจัยสำคัญที่ส่งผลต่อคุณสมบัติเชิงแสงของวัสดุนาโน ความแตกต่างของขนาดอนุภาคนาโนนั้นจะเป็นผลมาจากวิธีการและการควบคุมตัวแปรในการสังเคราะห์ วิธีการไมโครอิมัลชันเป็นวิธีการที่นิยมนำมาใช้ในการสังเคราะห์อนุภาคนาโน เนื่องจากใช้พลังงานต่ำและใช้อุปกรณ์ไม่ซับซ้อน อย่างไรก็ตามวิธีการนี้มักจะส่งผลให้อนุภาคนาโนมีการกระจายขนาดกว้าง ดังนั้นในการศึกษานี้จึงนำวิธีการไฮโดรไดนามิกคาวิเทชันมาใช้ในเตรียมไมโครอิมัลชันสังเคราะห์อนุภาคนาโน เพื่อให้สามารถควบคุมการกระจายขนาดได้ ระบบไมโครอิมัลชันประกอบด้วยน้ำ โซโคไลเฮกเซน เฮกเซนอล ไทรทัน X-100 และสารละลายของสารตั้งต้นที่กระจายตัวอยู่ ผลการทดลองแสดงให้เห็นว่า จำนวนรอบไหลวน หมายเลขคาวิเทชัน (C_v) และอัตราส่วนความเข้มข้นเชิงโมลของน้ำต่อสารตั้งต้นไทรทัน X-100 (W_0) ส่งผลอย่างมีนัยสำคัญต่อสมบัติการไหลและการกระจายขนาดของไมโครอิมัลชัน การเพิ่มจำนวนรอบไหลวนจาก 300 เป็น 1,500 รอบ สามารถลดขนาดเฉลี่ยของไมโครอิมัลชันลงได้ เนื่องจากความถี่ในการแตกตัวที่สูงขึ้น อันเป็นผลมาจากการกระจายพลังงานเข้าสู่ระบบที่มากขึ้น นอกจากนี้ C_v ที่สูงขึ้นนำไปสู่การลดขนาดของไมโครอิมัลชันลงได้ เนื่องจากความปั่นป่วนของการไหลที่สูงขึ้น ซึ่งได้รับการยืนยันโดยแบบจำลองพลศาสตร์ของไหลเชิงคำนวณ รวมถึงบทบาทของ W_0 ยังส่งผลต่อความหนาแน่น ความหนืด และแรงตึงผิวของไมโครอิมัลชัน พบว่าคุณสมบัติทั้งหมดมีค่าเพิ่มขึ้นอย่างมีนัยสำคัญเมื่อมีสัดส่วนของน้ำสูงขึ้น ขนาดเฉลี่ยเพิ่มขึ้นและการกระจายขนาดของไมโครอิมัลชันที่กว้างขึ้น จะเห็นได้ว่า ขนาดไมโครอิมัลชันที่แตกต่างกัน สามารถทำได้โดยการปรับ C_v และ W_0 ส่งผลให้อนุภาคนาโนสังกะสีซัลไฟด์ที่ก่อตัวอยู่ภายในไมเซลล์แบบย้อนกลับมีขนาดแตกต่างกันตามไปด้วย จากการวิเคราะห์ HRTEM อนุภาคนาโนสังกะสีซัลไฟด์ที่สังเคราะห์ได้นั้น มีลักษณะเป็นทรงกลมและขนาดเฉลี่ยที่เล็กที่สุดอยู่ 4.6 นาโนเมตร ที่เงื่อนไข C_v เท่ากับ 1.8 และ W_0 เท่ากับ 7 ผลการวิเคราะห์ XRD ยืนยันการก่อตัวของอนุภาคนาโนสังกะสีซัลไฟด์ เป็น โครงร่างผลึกทรงลูกบาศก์ ประเด็นสำคัญของการศึกษานี้ คือ การสร้างไมโครอิมัลชันจากวิธีไฮโดรไดนามิกคาวิเทชัน เป็นวิธีการที่มีศักยภาพ สามารถนำมาใช้ในการสังเคราะห์อนุภาคนาโนสังกะสีซัลไฟด์ที่ควบคุมขนาดได้โดยมีการกระจายขนาดที่แคบ และนำไปประยุกต์ใช้ในการผลิตอนุภาคนาโนในระดับอุตสาหกรรมในอนาคตได้

จุฬาลงกรณ์มหาวิทยาลัย
CHULALONGKORN UNIVERSITY

สาขาวิชา วิศวกรรมเคมี
ปีการศึกษา 2564

ลายมือชื่อ นิสิต
ลายมือชื่อ อ.ที่ปรึกษาหลัก
ลายมือชื่อ อ.ที่ปรึกษาร่วม

6270073721 : MAJOR CHEMICAL ENGINEERING

KEYWORD ZnS nanoparticles; Microemulsion; Hydrodynamic cavitation

D:

Nachapa Choojan : Synthesis of zinc sulfide nanoparticles using microemulsion generated by hydrodynamic cavitation method.
Advisor: Prof. TAWATCHAI CHARINPANITKUL, D.Eng. Co-advisor:
Dr. CHARUSLUK VIPHAVAKIT, Ph.D.

Zinc Sulfite (ZnS) nanoparticles have attracted attention of researchers as a promising material for semiconductor fabrication. Their optical properties are strongly size-dependent and related to production methodology. A microemulsion technique is simple and requires less energy to produce ZnS nanoparticles. However, this technique usually results in ZnS with a wide size distribution. In this work, microemulsion technique and hydrodynamic cavitation have been effectively combined for synthesis of ZnS nanoparticles with controllable and uniform size distribution. The microemulsion system which consists of water, cyclohexane, hexanol and Triton X-100 surfactant has been prepared by incorporating hydrodynamic cavitation. Experimental results number of passages, cavitation number (C_v) and water to surfactant molar ratio (W_0) exert significant effects on rheological properties and size distribution of microemulsion. Increasing number of passages from 300 to 1,500 passages could decrease average size of microemulsion due to higher breakage frequency, as number of passes represents energy dissipation in the system. Higher C_v led to reduction in microemulsion size, which was derived from high intensity turbulence, as confirmed by CFD modeling. Investigation on role of W_0 on density, viscosity and surface tension of microemulsions revealed that all properties significantly increased with higher water content. Moreover, average size also increased and size distribution of microemulsion became broader. Difference in microemulsion size would be achieved by adjusting C_v and W_0 , resulting in growth of ZnS nanoparticles with different size inside reverse micelles. Based on HRTEM analyses, the obtained ZnS nanoparticles exhibited spheroidal morphology and the smallest average size could be achieved at C_v of 1.8 and W_0 of 7. XRD analysis confirmed the successful formation of ZnS with cubic crystalline configuration. In summary, microemulsion method enhanced by hydrodynamic cavitation exhibits its potential in synthesis of ZnS nanoparticles with controllable size and narrow size distribution, which could be promising material in many applications.

Field of Study: Chemical Engineering

Student's Signature

Academic 2021

.....
Advisor's Signature

Year:

.....
Co-advisor's Signature

.....

ACKNOWLEDGEMENTS

I would like to express my sincere thanks to my thesis advisor, Professor Tawatchai Charinpanitkul, D.Eng. and my thesis co-advisor, Dr. Charusluk Viphavakit, PhD for profound belief in my abilities as well as helpful suggestions, patient guidance and inspirational encouragement from the beginning until the end of my study.

I am also grateful for the support and recommendation from Assistant Professor Apinan Sootittantawat, D.Eng. as the chairman, Assistant Professor Rungthiwa Methaapanon, PhD and Assistant Professor Prakorn Kittipoomwong, PhD as the members of the thesis committee.

I would like to offer my special thanks to Dr. Giang T. T. Le and all members of Prof. Tawatchai's research group for their helpful contributions throughout my study.

I would like to show my deep gratitude to the Center of Excellence in Particle Technology and Material Processing – CEPT, and Ratchadapisek Somphot fund, Chulalongkorn University, for the financial supports of this project.

I am also thankful to all members of the CEPT for their warm collaborations and kindness during my thesis work.

Finally, I would like to dedicate this work with my cordial and deep thanks to my family for their unconditional love and encouragement for me.

TABLE OF CONTENTS

	Page
ABSTRACT (THAI)	iii
ABSTRACT (ENGLISH).....	iv
ACKNOWLEDGEMENTS	v
TABLE OF CONTENTS.....	vi
LIST OF TABLES	ix
LIST OF FIGURES	x
CHAPTER 1 INTRODUCTION.....	12
1.1 Rationale and motivation.....	12
1.2 Research Objectives.....	14
1.3 Scopes of Research	14
1.4 Expected benefits	15
CHAPTER 2 FUNDAMENTAL THEORY AND LITERATURE REVIEWS.....	16
2.1 Hydrodynamic cavitation for preparation of microemulsions.....	16
2.2 Microemulsion method for nanoparticles synthesis	19
2.3.1 General aspects of microemulsions.....	19
2.3.2 Nanoparticles synthesis prepared in water-in-oil (W/O) microemulsions.....	20
2.3.3 Parameters related to the size of reverse micelle in microemulsion	22
2.3 Physical properties of zinc sulfide nanoparticles.....	23
2.4 Literature reviews	25
CHAPTER 3 EXPERIMENTAL AND ANALYTICAL TECHNIQUE	31
3.1 Experimental setup	31
3.2 ZnS nanoparticles synthesis using microemulsion generated by hydrodynamics cavitation	32
3.3 Analytical technique	33
3.3.1 Rheological properties of ZnSO ₄ microemulsion	33
3.3.2 Dynamic Light Scattering (DLS)	33

3.3.3 Transmission electron microscopy (TEM).....	34
3.3.4 X-ray diffractometer (XRD).....	34
3.4 Computational fluid dynamics (CFD) modeling	35
CHAPTER 4 RESULTS AND DISCUSSION.....	38
4.1 Characteristic of relevant substances	38
4.2 Investigation of properties and size distribution of microemulsion prepared by hydrodynamic cavitation	40
4.2.1 Effect of number of passages on size distribution of microemulsion	40
4.2.2 Effect of cavitation number on size distribution of microemulsion	43
4.2.3 Effect of water to surfactant molar ratio on size distribution of microemulsion	48
4.3 Investigation of size distribution and morphologies of ZnS nanoparticles synthesized by microemulsion	53
4.3.1 Yield of synthesized ZnS nanoparticles	53
4.3.2 Morphologies and size distribution of ZnS nanoparticles.....	56
4.3.3 Crystalline structure of ZnS nanoparticles	59
CHAPTER 5 CONCLUSIONS AND RECOMMENDATIONS	63
5.1 Conclusions.....	63
5.1.1 Preparation of microemulsion by hydrodynamic cavitation	63
5.1.2 ZnS synthesis by microemulsion method enhance by hydrodynamic cavitation	64
5.2 Recommendations.....	66
REFERENCES	67
APPENDIX.....	73
APPENDIX A CALCULATION	74
APPENDIX B AVERAGE SIZE AND SIZE DISTRIBUTION OF MICROEMULSION.....	76
APPENDIX C YIELD OF SYNTHESIZED ZNS NANOPARTICLES	81
APPENDIX D TEM IMAGES OF ZNS NANOPARTICLES.....	82
APPENDIX E EDX SPECTRUM OF TYPICAL ZNS NANOPARTICLES	85

APPENDIX F SCHEMATIC DIAGRAM AND DIMENSION OF THE
EXPERIMENTAL SETUP86
VITA87



LIST OF TABLES

	Page
Table 1 Average size and standard deviation of ZnSO ₄ and Na ₂ S microemulsion.....	42
Table 2 The crystalline size of ZnS nanoparticles	60



LIST OF FIGURES

	Page
Figure 1 Schematic diagram of the pressure variations in the hydrodynamic cavitation [18].....	17
Figure 2 Microemulsion preparation by HC.....	18
Figure 3 The formation of water-in-oil (W/O) emulsion and oil-in-water (O/W) emulsion.....	20
Figure 4 A typical structure of reverse micelle [3].....	21
Figure 5 Mechanism of the formation of nanoparticles [3].....	21
Figure 6 Effect of W_0 on size of reverse micelles in microemulsions [23].....	22
Figure 7 Models showing the zinc blende and wurtzite crystal structures [25].....	23
Figure 8 Effect of inlet pressure and cavitation number on droplet size [8].....	25
Figure 9 Effect of number of passages on droplet size [2].....	26
Figure 10 TEM images of ZnS nanoparticles synthesized at: (a) $W_0=7$, (b) $W_0=11$ [13].....	27
Figure 11 The fluorescence image of ZnS nanoparticles: (a) without excitation and (b) excited with 330 nm [29].....	28
Figure 12 The fluorescence image of ZnS: Mn excited with 450 to 490 nm wavelength [29].....	28
Figure 13 The fluorescence image of ZnS: Mn excited with 450 wavelengths [29]...29	29
Figure 14 HRTEM images of the prepared CdS: (a) stirring, 30 min and (b) sonication, 30 min.....	30
Figure 15 The schematic diagram of the experimental setup.....	31
Figure 16 Zetasizer (MALVERN Zetasizer Nano ZSP).....	34
Figure 17 XRD (BRUKER D8 DISCOVER).....	35
Figure 18 Meshed geometry.....	37
Figure 19 Rheological properties of $ZnSO_4$ microemulsion prepared with different W_0	40
Figure 20 Energy dissipated into the system and average size of $ZnSO_4$ microemulsion.....	42

Figure 21 Contour of velocity magnitude (m s^{-1}) and turbulent kinetic energy ($\text{m}^2 \text{s}^{-2}$) at different Cv	44
Figure 22 Effect of Cv on size distribution of microemulsions with a difference in the number of passages	46
Figure 23 Average size of microemulsion with difference in Cv of (a) ZnSO_4 microemulsion and (b) Na_2S microemulsion	47
Figure 24 Rheological properties and Re of ZnSO_4 microemulsion prepared with different W_0	48
Figure 25 Effect of water to surfactant molar ratio on size distribution of microemulsion with difference in number of passages.....	51
Figure 26 Average size of microemulsion with difference in W_0 (a) ZnSO_4 microemulsion and (b) Na_2S microemulsion	52
Figure 27 Yields of weight of synthesized product at: (a) various Cv and (b) various W_0	55
Figure 28 TEM micrograph and size distribution of ZnS nanoparticles	57
Figure 29 XRD patterns of ZnS nanoparticles	60
Figure 30 HRTEM and SAED image of ZnS nanoparticles at Cv of 1.8 and W_0 of 15	61

CHAPTER 1

INTRODUCTION

1.1 Rationale and motivation

Recently, nanostructured materials have drawn great attention due to their extensive applications in various fields in our daily life, including household, cosmetics, textiles, energy storage and catalyst. In addition, nanoparticles have shown potentials for photonic, optical, and electronic device fabrication. Zinc Sulfite (ZnS) nanoparticles have attracted particular attention as promising material for fabricating semiconductor. Semiconductor materials exhibit remarkable photoelectrochemical properties due to their quantum size and unique surface morphologies. Several strategies have been successfully developed to obtain quantum-sized nanocrystals [1]. There are various methods for the synthesis of ZnS nanoparticle such as thermal reactions, solution method in a polyol, solution-phase decomposition and microemulsion method [2].

In recent years, microemulsions approach has been widely considered for nanoparticles preparation. Water in oil (W/O) microemulsion that is thermodynamically stable has been introduced to ZnS synthesis. W/O microemulsion could be prepared from at least three components, comprising two immiscible liquids, and stabilized by surfactant and cosurfactant. These stabilizers play important role in nanoparticles synthesis as they strongly influence the properties of as-produced nanoparticles [3, 4]. The advantage of the microemulsion-based route is that uncomplicated equipment and non-requirement of handling any poisonous gas [5]. However, this method is not suitable for the industrial-scale production of nanomaterials, which could be due to the use of large-scale reactors for large quantities of produced nanoparticles products. Moreover, it is difficult to control the size of particles within a nanoscale by using the conventional synthesis method (stirrer). The formed nanoparticles by this method are larger and also exhibit broader droplet size distribution. [6].

Preparation of microemulsions by hydrodynamic cavitation method is a newly developed process. It can be achieved by different system geometries, such as venturi tube, throttling valve, and multi-nozzles, [7] which affect pressure variations in a

flowing liquid as a liquid mixture flow passes through the constriction of a pipe [8]. This approach can be used for controlling the size of emulsion to a nanoscale and narrowing size distribution for the formation and growth of crystallized nanoparticles in the liquid medium. It also delivers other advantages such as easy handling, less energy consumption than other methods for microemulsion preparation.

Several studies have been conducted to obtain micro or nano-sized emulsion [6, 9]. Generally, the size distribution of microemulsion can be intensively influenced by modifying the energy input or emulsification time [9, 10], in which droplet size is a particularly important factor to prepare nanostructures with smaller size. For the synthesis of ZnS nanoparticles, Jovanović et al. reported that synthesizing ZnS nanoparticles with cubic zinc blende crystal structure in W/O microemulsions was successful. [11]. Similarly, Charinpanitkul et al. could obtain ZnS nanoparticles in a narrow size distribution by varying the molar ratio of water to surfactant (W_0) within the range of 7.0-20.0. Both of Triton X-100 and n-hexanol have been employed as surfactant and co-surfactant, respectively. The as-synthesized ZnS nanoparticles products with the use of Triton X-100 and n-hexanol have exhibited superior properties than that obtained in the absence of them [12, 13]. The uniformity of shape and smaller size are challenging problem to develop synthesis method for ZnS nanoparticles. The downsizing of the synthesized product can improve the performance for specific applications such as efficient photocatalysts for removing pollutants from wastewaters and faster response transistors in the microelectronics fields [12, 14]. There is no work reported in the literature on the preparation of microemulsion and optimization of operating variables for ZnS synthesis by hydrodynamic cavitation.

In this work, a novel technical route was used to prepare ZnS nanoparticles. Microemulsion technique and hydrodynamic cavitation using multi-nozzles were effectively combined for the synthesis of ZnS nanoparticles. Cavitation number was studied to comprehend the effect of superficial velocity of the circulated microemulsion on the microemulsion characteristic. CFD model was employed to predict the behavior of microemulsion in the tank and to understand interaction between turbulence intensities and size distribution. Also, water to surfactant molar ratios was investigated to discuss the rheological properties of microemulsion which

in turn affects the collision of microemulsion and formation of ZnS within the reverse micelles. Finally, size distribution, morphology and crystalline structure of the resultant ZnS nanoparticles were also examined by transmission electron microscope and X-ray diffractometer.

1.2 Research Objectives

This work aims to synthesize ZnS nanoparticles using a novel microemulsion enhanced by hydrodynamic cavitation method. Effects of cavitation number, and water to surfactant molar ratio on size and properties of microemulsion and the resultant ZnS are investigated.

1.3 Scopes of Research

1. Design the experimental method to prepare reversed micelles microemulsion generated by multi-nozzle
2. Synthesize ZnS nanoparticles using microemulsion technique prepared by hydrodynamic cavitation method using the following conditions
 - Cavitation number for microemulsion preparation: 1.8, 3.2 and 7.1
 - Molar ratio of water to surfactant ($W_0 = [\text{H}_2\text{O}]: [\text{Triton X-100}]$): 7, 11 and 15 (Reactant concentration = 0.1 mol/dm^3 and a concentration ratio of $C_{\text{Triton X-100}}/C_{\text{n-hexanol}} = 1$)
3. Characterize the relevant substances as following:
 - Rheological properties of ZnSO₄ microemulsion: viscometer (SV-10, A&D Company, Limited, Japan) and Tensiometer (DCAT11, Data Physics Instruments, Germany)
 - Size distribution of ZnSO₄ and Na₂S microemulsion; Zetasizer (Zetasizer Nano ZSP, MALVERN, UK) with providing dynamic light scattering method
4. Characterize the synthesized ZnS nanoparticles with the following techniques:
 - Morphology and size distribution of the synthesized ZnS: transmission electron microscope (TEM JEM-2100, JEOL Ltd., Japan)
 - Crystalline of the synthesized ZnS: X-ray powder diffractometer (D8 Discover, Bruker, Germany)

1.4 Expected benefits

1. Knowledge of synthesis ZnS nanoparticles in microemulsion using hydrodynamic cavitation method
2. Better understanding on the effects of operating variables on characteristics of ZnSO₄ and Na₂S microemulsion for ZnS nanoparticles synthesis
3. Knowledge of controllable sizes of ZnS nanoparticles by varying cavitation number and water to surfactant molar ratio



CHAPTER 2

FUNDAMENTAL THEORY AND LITERATURE REVIEWS

This chapter aims to give basic knowledge on hydrodynamic cavitation for microemulsion preparation. It also described the use of microemulsions for synthesizing and outlines the major factors responsible to control the sizes and morphology of these nanoparticles. Simultaneously, the recent research on the synthesis of ZnS nanoparticles using this method was summarized.

2.1 Hydrodynamic cavitation for preparation of microemulsions

In recent years, hydrodynamic cavitation (HC) has been recognized as a novel and attracted technique that developed for process intensification, which is expected to contribute for emulsion formation in large scale.

Hydrodynamic cavitation is induced by sudden change of pressure in a flowing fluid passes through a constricted part such as venturi tubes, orifice plates, a throttling valve, multi-nozzle. According to Bernoulli's principle, the reduction of the flow area results in the flow velocity rises and the pressure is reduced below the vapor pressure, which includes generation of cavities and fragmentation of the droplets into smaller size [15]. The change of pressure in a flowing liquid in the form of a Venturi tube based on the hydrodynamic cavitation phenomenon is depicted in **Figure 1**.

When liquid passes through the constricted part, boundary layer separation occurs and local turbulence results in a substantial loss of energy in the form of permanent pressure drop; and lowest local pressure subsequently occurs inside the smallest cross-section area, that called 'vena contracta'. After that, at downstream of the constriction, the intensity of fluid turbulence is generated. The cavitation intensity is typically dependent on the intensity of turbulence [16, 17].

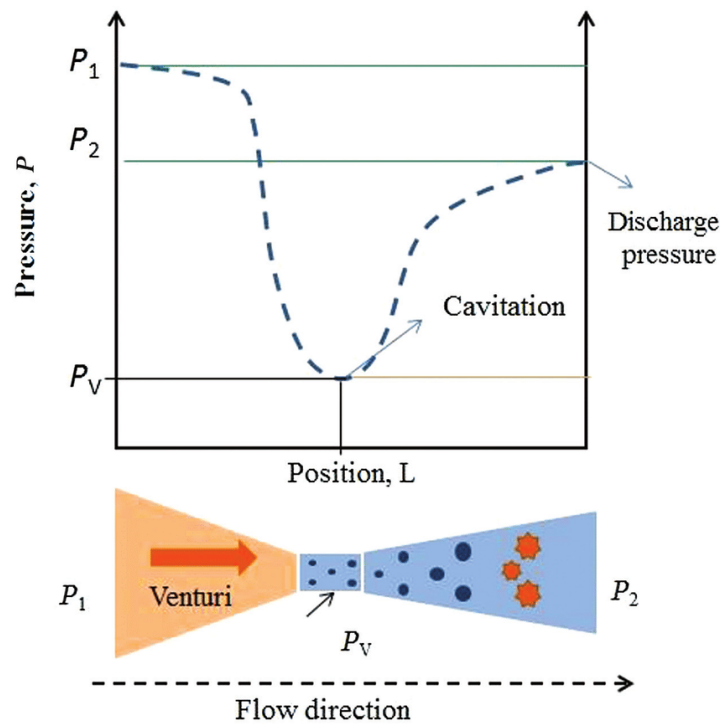


Figure 1 Schematic diagram of the pressure variations in the hydrodynamic cavitation [18]

The pressure–velocity relationship of the flowing fluid in hydrodynamic cavitation is well described by Bernoulli’s equation presented in **Equation 1**

$$P_1 + \frac{1}{2}\rho v_1^2 + \rho g h_1 = P_2 + \frac{1}{2}\rho v_2^2 + \rho g h_2 \quad (1)$$

where,

P_1 is the upstream bulk pressure (N m^{-2}),

P_2 is the pressure at the nozzle (N m^{-2}),

ρ is the fluid density (kg m^{-3}),

v_1 and v_2 are the superficial velocity of the circulated microemulsion (m s^{-1}),

h_1 and h_2 are the heights of the fluid (m),

g is gravity (m s^{-2}).

Considering the extended Bernoulli-equation, the second term at each side of **Equation 1** represents the specific kinetic energy while the third term represents the specific potential energy. The mechanical energy conservation equation for moving fluid is expressed by **Equation 1**. Assuming equal heights, fluid acceleration due to

mass conservation ($v_2 > v_1$) results in arises the pressure drop ($P_2 < P_1$) at the reactor's nozzle.

The performance comparison of the cavitating devices is represented by a dimensionless number known as the cavitation number (C_v) which is derived from Bernoulli's equation. Cavitation number can be used to characterize the cavitation intensity in the flow conditions which is defined as **Equation 2**.

$$C_v = \frac{P_2 - P_v}{\frac{1}{2}\rho v^2} \quad (2)$$

where,

P_2 is the fully recovered downstream pressure (N m^{-2}),

P_v is the vapor pressure of the aqueous solution (N m^{-2}),

ρ is the density of the aqueous solution (kg m^{-3}),

v is superficial velocity of the circulated microemulsion (m s^{-1}).

Cavitation number relates the ratio between the pressure drop needed to achieve vaporization and the specific kinetic energy at the cavitation inception section [19]. In general, the collapse of cavitation is known to have significant effect on droplet breakup during emulsification (**Figure 2**). Water and oil are inherently immiscible. However, these two liquids could be emulsified into a heterogeneous mixture of one micro-particle liquid phase dispersed into another liquid phase by mechanical blending [20]. One type of injection system by multi-nozzles has been used to produce emulsions of water/oil (W/O) type, where the emulsion component is injected by means of a multi-nozzle submerged in quiescent waters, into which water is introduced tangentially to the axis of the atomizer. Water droplets flowing out through holes with relatively small diameters are “cut off” due to the swirling motion of the water stream, and are thus separated from the injector [21].

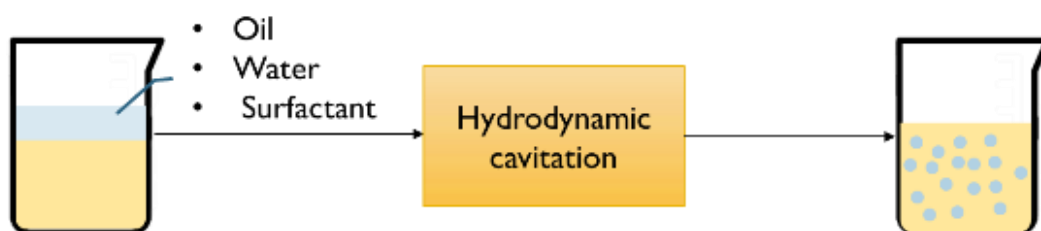


Figure 2 Microemulsion preparation by HC

2.2 Microemulsion method for nanoparticles synthesis

The synthesis of well-defined nanoparticles with controlled sizes and shapes is important for the development of novel technologies. This section aims to give a vivid look at the use of the emulsion methods for the synthesis of nanoparticles and the major factors responsible for controlling of sizes and shapes of nanoparticles.

2.3.1 General aspects of microemulsions

Microemulsions are emulsions with droplet size in the micrometer range. An emulsion, by definition, is an optically transparent and thermodynamically stable system composed of a mixture of water (polar phase)/oil (nonpolar phase)/surfactants and co-surfactants in a sufficient quantity to obtain microdroplet. Microemulsion consists of two phases: one with the continuous medium and another one is the dispersed phase. The dispersed phase is the phase broken into fine droplets while the continuous medium is liquid surrounding the droplets. The formation of the dispersed phase can lead to the formation of oil-in-water (O/W) emulsion or water-in-oil (W/O) emulsion as show in **Figure 3**. The latter can be used as nanoreactors for the synthesis of nanoparticles which is the major focus of this section [22].



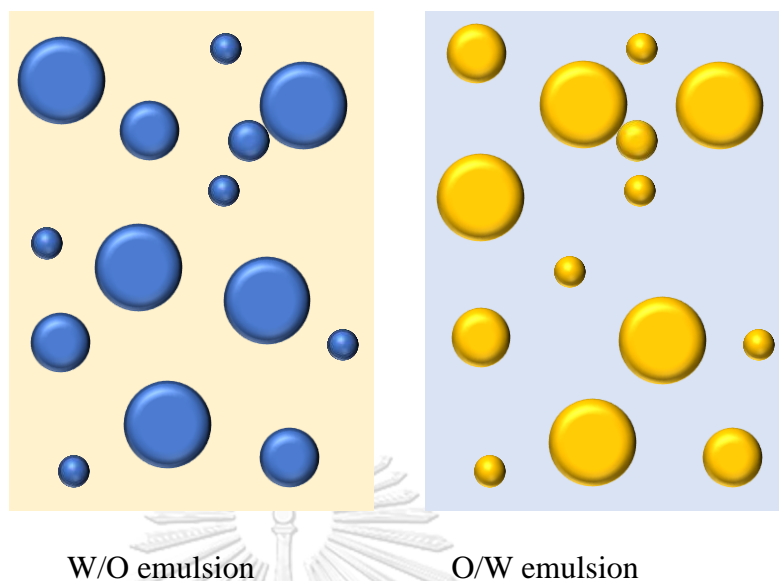


Figure 3 The formation of water-in-oil (W/O) emulsion and oil-in-water (O/W) emulsion

2.3.2 Nanoparticles synthesis prepared in water-in-oil (W/O) microemulsions

The use of microemulsions for the synthesis of nanoparticles called Emulsion method (also called as reverse micellar route). This is one of the bottom-up approaches that yield nanostructured materials with monodisperse size distribution.

A water-in-oil microemulsions is formed when water is dispersed in a hydrocarbon based continuous phase. Surfactant molecules are dissolved in organic solvents to form spheroidal aggregates known as reverse micelles. The polar head groups of surfactants could point inwards or towards the core (**Figure 4**). These microdroplets can be used as nanoreactors to carry out chemical reactions, providing a suitable environment for controlled nucleation and growth [3].

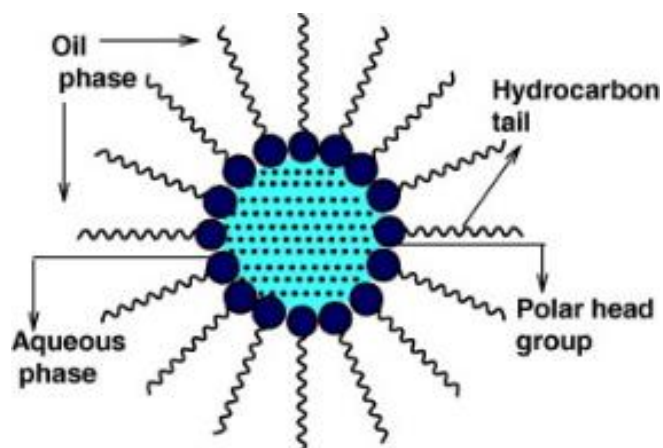


Figure 4 A typical structure of reverse micelle [3]

In order to synthesis the nanoparticles, W/O microemulsions contains two reactants A and B (in separate emulsions) carrying the water-soluble reactants, which are dispersed in the continuous medium are mixed as shown in **Figure 5** [3]. The Brownian motion of the micelles leads to inter-micellar collisions. The reactants are exchanged and reacted through the process of coalescence. The chemical reaction starts when the collision of the micelles. The micelles undergo numerous collisions results in nuclei formation and thereby leads to the growth of nanoparticles.

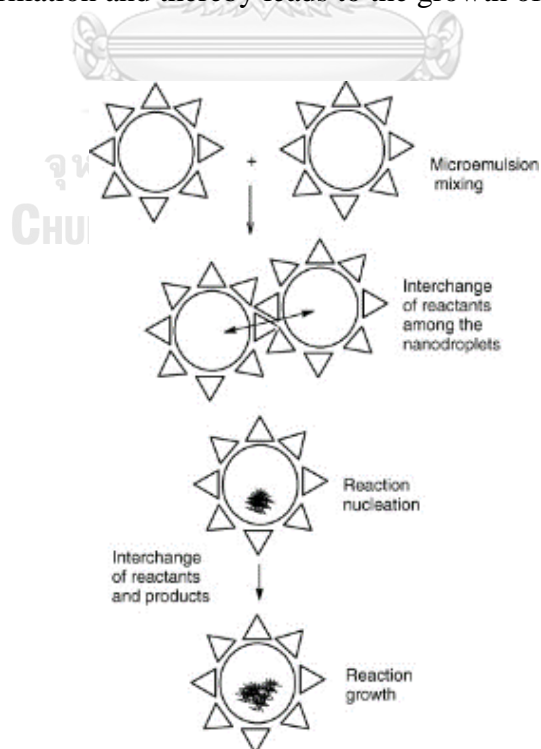


Figure 5 Mechanism of the formation of nanoparticles [3]

2.3.3 Parameters related to the size of reverse micelle in microemulsion

The research carried out in the last few years has shown that several parameters such as water to surfactant ratio (W_0), nature of surfactant, nature of the solvent and the nature of co-surfactant also play important roles in fluorescence properties of the final product [23].

Effect of water to surfactant ratio (W_0)

If water content is varied while amount of surfactant is kept constant, the size of reverse micelle could be distinctly affected as shown in **Figure 6**. Hence, change in W_0 has a direct effect on the size of the final product obtained. The study on the effect of the amount of water on the size of CuC_2O_4 nanoparticles shows that the size of these was 30–50 nm at $W_0=11$, 50–60 nm at $W_0=14$ and 80–100 nm at $W_0=16$. It can be explained by surfactant film rigidity. As W_0 increases, the size of reversed micelles also increases resulting in the decrease of rigidity of the surfactant film. This effect result in a faster interdroplet exchange rate leading to an increase in the size of nanoparticles [23].

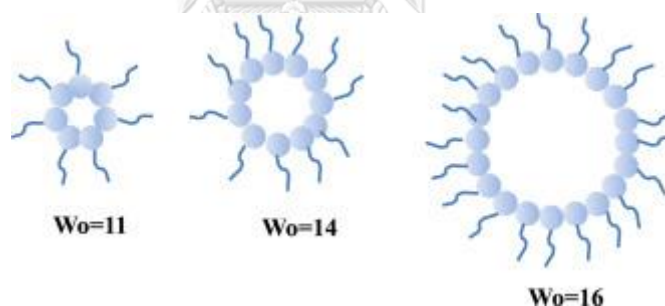


Figure 6 Effect of W_0 on size of reverse micelles in microemulsions [23]

Effect of surfactant

Surfactant is a material that plays a critical role on the flexibility of the reverse micelles. With surfactants, emulsions are mixed well and have high stability. In case of non-ionic surfactants, the particles are capped in all directions resulting in uniform growth. The type of polar head group of cationic surfactants results in the change of surface charge to a positive value leading to the formation of nanoparticles along axis or rods [23].

Effect of co-surfactant

Generally, alcohols or amines short chain have been used as co-surfactants for nanoparticles synthesis. It helps in changing the curvature of the reverse micelles. The chain length of the co-surfactant increases result in the curvature increases and hence leads to decrease in the interdroplet exchange rate [23].

2.3 Physical properties of zinc sulfide nanoparticles

Zinc sulfide is an inorganic compound generally in white powder form with dimension in 1–100 nm range. Zinc sulfide (ZnS) can exist in nature or from synthetic approach with two types of crystalline structures: zinc blende and wurtzite structure. The cubic structure is stable at low temperature. At high temperatures around 1296 K, the cubic zinc blende structure can transform to hexagonal wurtzite structure as shown **Figure 7** [24, 25].

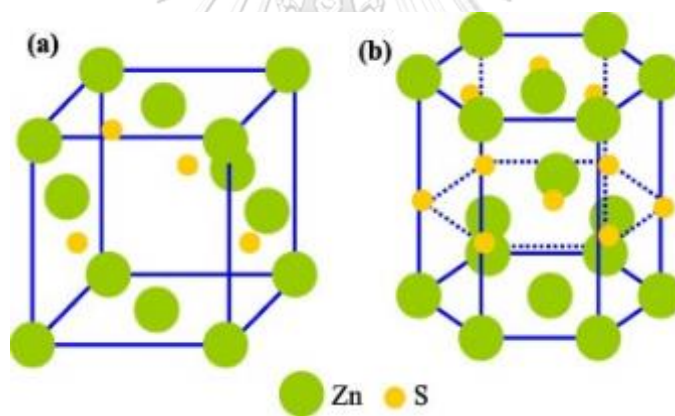


Figure 7 Models showing the zinc blende and wurtzite crystal structures [25]

The difference in atomic arrangements results in different electronic structures and bandgaps. The band structure of a solid material is the range of energy that an electron can move independently from the valence band (VB) to the conduction band (CB). Zinc blende and hexagonal wurtzite structure have a bandgap of approximately 3.72 eV and 3.77 eV, respectively, and it determines the distinct optical properties of zinc sulfide nanoparticles.

The ZnS nanoparticle can be categorized as 0D, 1D, and 2D dimension depending on their shapes [26].

0D nanostructures (0D nanocrystals): also called quantum dots (QDs). QDs have a diameter of less than 100 nm which are quasi-spherical particles. QDs have particularly interesting structural properties such as ultra-small sizes and high surface-to-volume ratios, they have more active edge sites per unit mass [27]. Quantum dots have proven to be high photoluminescence (PL) quantum efficiency and chemiluminescence because of the edge and quantum confinement effects. With such novel particular properties, ZnS QDs have become the great adaptability ideal for various applications, especially those based on optical applications or electroluminescent exploration, infrared windows, photovoltaics, dielectric filters [25].

1D nanostructures: 1D nanostructures nanoparticles are one of the most interesting and widely researches in recent years in the fields of basic scientific research and potential technological applications. ZnS can be ideal for nanoscale devices such as electromechanical, optoelectronic, fabricating electronic and electrochemical devices. Generally, 1D nanostructures can be classified into various types: nanotubes, nanorods, nanowires and nanobelts.

Typically, ZnS nanotubes have perfectly straight and hexagonal or circular cross-section morphologies. Nanorods have a circular or hexagonal cross-section prevalent shorter and therefore stiffer. Nanowires have a circular cross-section, relatively long and flexible. ZnS nanobelts or nanoribbons have rectangular cross-sections geometry, high-crystallinity and flexibility [28].

2.4 Literature reviews

Various methods for preparation of emulsion by hydrodynamic cavitation method have been studied. Among all parameter, the effect of flow rate and circulation time on the characteristics of emulsion have been reported as follows.

George et al. (2017) conducted experiments on mustard oil in water nanoemulsion [8]. This experiment was aimed to determine the effect of cavitation number and inlet pressure on the reduction of droplet size when using mustard oil in water. The emulsification process was prepared using hydrodynamic cavitation with surfactants. As shown in **Figure 8**, a distinct decline in droplet size could be attained when increasing the pressure from 5 to 10 bar but no further reduction or in only a marginal droplet size on further increasing the pressure from 10 to 15 bar was observed. The study results also showed that increasing the inlet pressure, consequently decreased the cavitation number (C_v) due to the velocity at the throat increased as per the definition in **Equation 2**. Hence, the enhancement of turbulence and shear obtained at lower C_v resulted in the droplet size reduced.

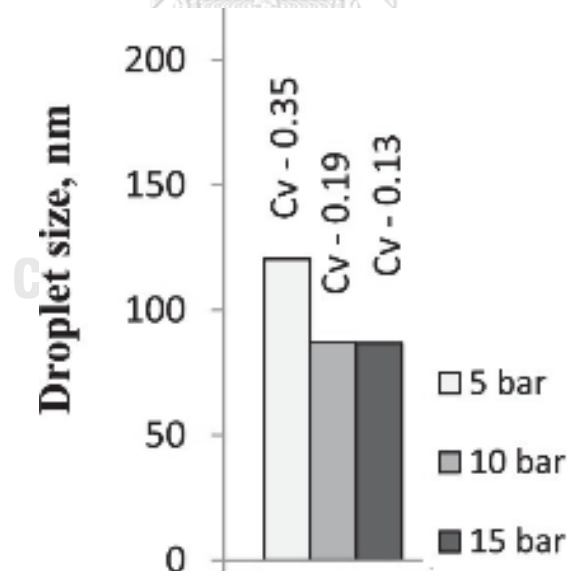


Figure 8 Effect of inlet pressure and cavitation number on droplet size [8]

Zhang et al. (2016) reported the formation of sub-100 nm oil-in-water (O/W) emulsions by hydrodynamic cavitation method [2]. In this work, refined soybean oil was used to prepare O/W emulsions. The effects of the number of passages on the

droplet size of emulsions was investigated in detail. This experiment proved that the emulsion could be successfully formed by hydrodynamic cavitation emulsification with average droplet size of about 100 nm. The results showed that the number of passages could affect droplet size reduction. As shown in **Figure 9**, there was a noticeable decline in droplet size when the number of cavitation passes increased from 1 to 6 passes. Increasing the number of cavitation passes resulted in a reinforcement of the intensity of turbulence, consequently the average droplet sizes of the O/W emulsions were decreased [6].

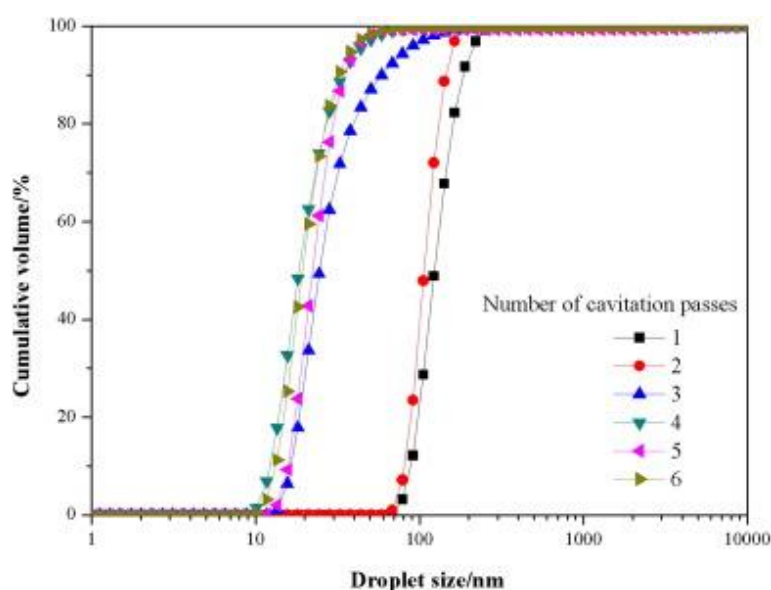


Figure 9 Effect of number of passages on droplet size [2]

Charinpanitkul et al. (2005) investigated effect of molar ratio of water to surfactant (W_0) on the synthesis of ZnS nanoparticles by microemulsion method. In this work, the effect of W_0 on morphology of ZnS nanoparticles was experimentally examined using Triton X-100 as surfactant and n-hexanol as cosurfactant. The employed W_0 values were 7 and 11 while the remaining parameters were fixed. The study results showed the morphology of products could be controlled by adjustment of W/O. The morphology of the synthesized ZnS are quantum dots. At $W_0=7$, the size of ZnS was 40–100 nm. On the other hand, increasing W_0 value to 11:1 could result in larger diameters as shown in **Figure 10** [13].

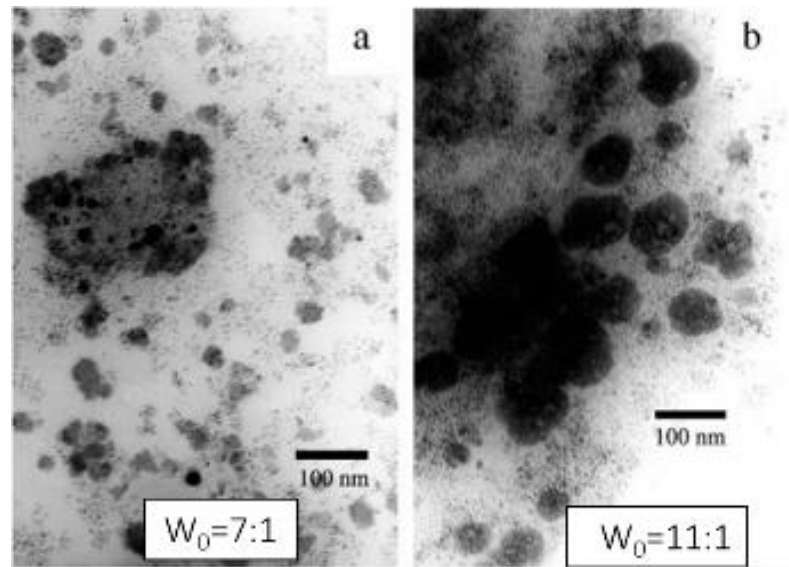


Figure 10 TEM images of ZnS nanoparticles synthesized at: (a) $W_0=7$, (b) $W_0=11$
[13]

Ma et al. (2011) conducted the synthesis of pure ZnS and ZnS: Mn nanoparticles by a facile hydrothermal method. The optical properties were changed by Mn ions due to impurity level. ZnS and ZnS: Mn nanocrystals were observed with a fluorescence microscope. The image of ZnS nanoparticles without excitation is shown in **Figure 11 (a)**, exhibiting the aggregation of small nanoparticles with diameter of 200 nm to form ZnS cluster. The bright blue fluorescence light (**Figure 11 (b)**) was emitted and correspond to those of the ZnS clusters. For ZnS: Mn nanocrystals, a bright yellow with bluish was observed, as shown in **Figure 12**. The yellow PL is enhanced. A slight addition of doped-Mn in the sample could lead to the emission of super-bright yellow fluorescence light, as shown in **Figure 13**. The super-bright ZnS: Mn nanoparticles could be employed as fluorescence powder in making LED and plat display without any damage to mankind and environment [29].

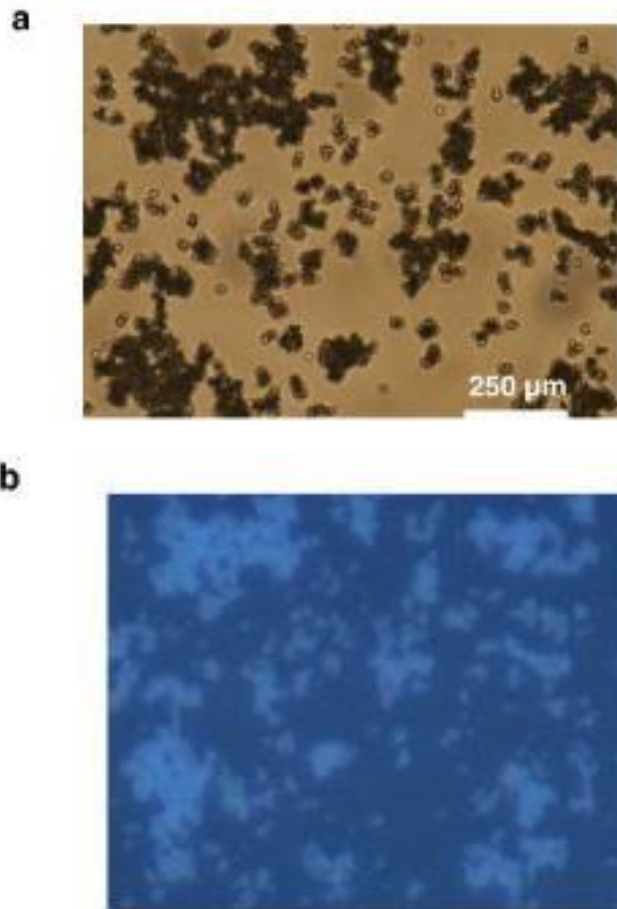


Figure 11 The fluorescence image of ZnS nanoparticles: (a) without excitation and (b) excited with 330 nm [29]

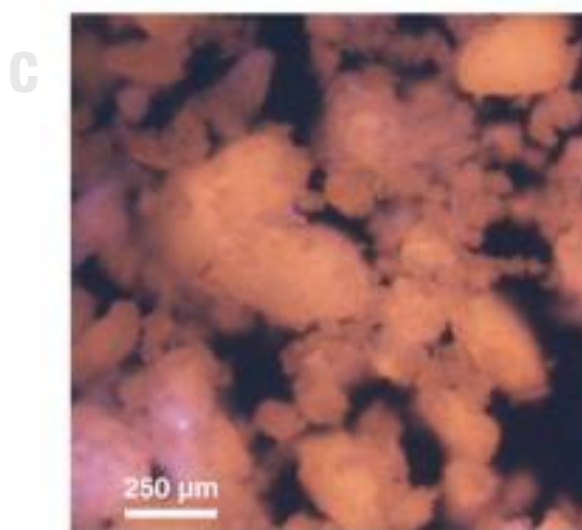


Figure 12 The fluorescence image of ZnS: Mn excited with 450 to 490 nm wavelength [29]

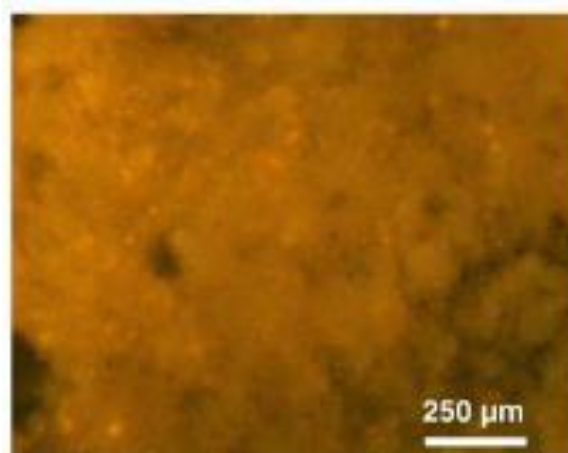


Figure 13 The fluorescence image of ZnS: Mn excited with 450 wavelengths [29]

Entezari et al. (2011) studied several influential factors such as sonication time, ultrasound intensity, temperature, and oil fraction on the formation of CdS nanoparticles in microemulsion. The microemulsion was prepared with ultrasound in two separate parts. During sonication, many nuclei were formed immediately, and temperature was increased from 30 to 60 °C. After that, both microemulsions were mixed by stirring. The uniform spherical morphology and small sizes of CdS nanoparticles are shown in **Figure 14 (a)** and **(b)**. The size and the surface area of CdS nanoparticles are related to sonication time. Ultrasound can decrease the particle size because it causes significant effect on the nucleation process of CdS nanoparticles [30].

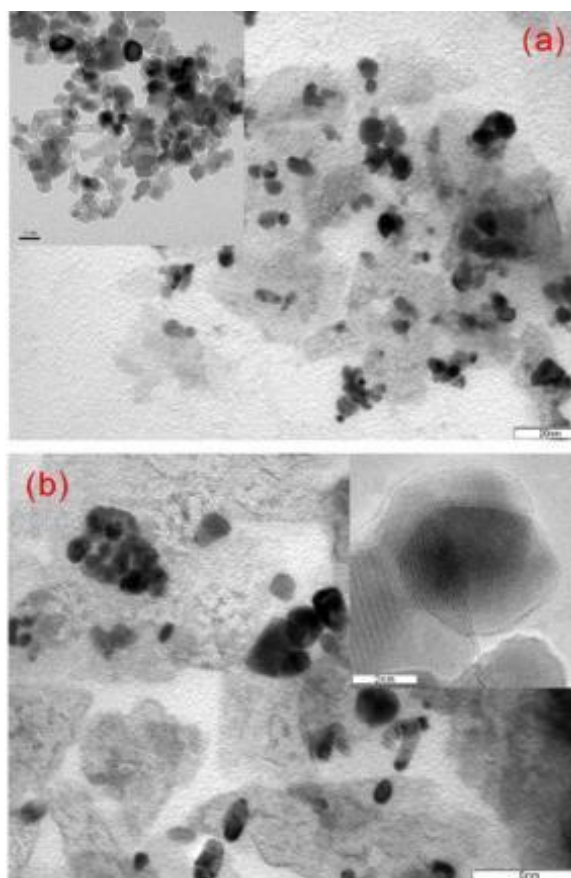


Figure 14 HRTEM images of the prepared CdS: **(a)** stirring, 30 min and **(b)** sonication, 30 min

This chapter provides the basic knowledge of the synthesis route in water-in-oil (W/O)-microemulsion and major aspects of microemulsion based synthesis which can be manipulated for controlling the size and morphology of the final product. Based on several studies, the hydrodynamic cavitation method via microemulsion route has exhibited its potential for ZnS synthesis with controllable size in nanoscale. Therefore, this work would focus on the effects of influential factors such as cavitation number, water to surfactant molar ratio on characteristics of microemulsion and ZnS as described and discussed in the following chapters.

CHAPTER 3

EXPERIMENTAL AND ANALYTICAL TECHNIQUE

This chapter is conducted to investigate the microemulsion preparation by hydrodynamics cavitation method together with mechanism of ZnS nanoparticles formation using various analytical techniques. In this work, the experiments can be divided into four parts. The first part is experimental setup. The second part is ZnS nanoparticles synthesis using microemulsion generated by hydrodynamics cavitation method. The third part is analytical technique. In characterization part, all the synthesized ZnS nanoparticles would be characterized by X-Ray diffraction spectroscopy (XRD) and transmission electron microscopy (TEM). The last part is simulation which is used to describe and predict microemulsion behavior.

3.1 Experimental setup

The schematic diagram of experimental setup for conducting emulsification process is shown in **Figure 15**. A vessel with capacity 1 dm³ was employed. The base of the vessel was connected to the suction side of a magnetic gear pump (MD-70R, Iwaki Co. Ltd., Japan) which discharges the solution to a multi-nozzle in the outlet. The hydrodynamic cavitation could be generated by a multi-nozzle (stainless steel 304) including 24 holes with diameter of 1 mm.

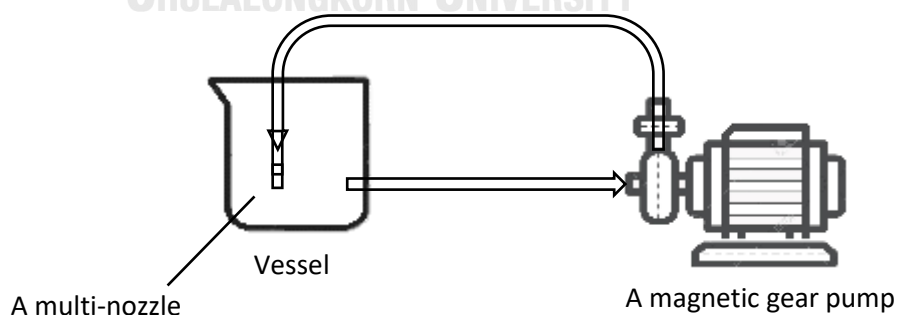


Figure 15 The schematic diagram of the experimental setup

3.2 ZnS nanoparticles synthesis using microemulsion generated by hydrodynamics cavitation

Microemulsion system consisting of cyclohexane, Triton X-100, n-hexanol were purchased from Sigma-Aldrich whereas zinc sulfate ($\text{ZnSO}_4 \cdot 7\text{H}_2\text{O}$, >99.5%) was from Ajax Finechem and sodium sulfide ($\text{Na}_2\text{S} \cdot 9\text{H}_2\text{O}$, >98%) is from Rankem (India).

At first, the solution containing 500 ml of cyclohexane (oil phase) and Triton X-100 (surfactant) and n-hexanol (cosurfactant) were circulated pass through the multi-nozzles for 100 passages at C_v of 1.8, 3.2 and 7.1 (flow rate 12, 9 and 6 L/min) (a concentration ratio of $C_{\text{TritonX-100}}/C_{\text{n-hexanol}} = 1$). After that, the aqueous solution of ZnSO_4 or Na_2S was slowly dropped in the system and circulated. The reactant concentration is kept constant at 0.1 mol/dm³. The molar ratio between water and surfactant was varied of 7, 11 and 15 ($W_0 = [\text{H}_2\text{O}]: [\text{Triton X-100}]$). The samples were collected at every 300 passages interval following **Equation 3** and then analyzed for the droplet size. The W/O microemulsion is formed after the mixture passed through the multi-nozzle. Two types of microemulsion system containing ZnSO_4 or Na_2S were mixed for 100 passages and then rested for 24 h at room temperature. Finally, the precipitate was separated by a centrifuge and then washed with ethanol three times and dried at 100 °C for 3 h. The final product was called ZnS nanoparticles.

$$\text{Number of passages} = \frac{\text{Volumetric flow rate}}{\text{Total volume of emulsion}} \times \text{circulation time} \quad (3)$$

3.3 Analytical technique

3.3.1 Rheological properties of ZnSO₄ microemulsion

Viscosity of each microemulsion was analyzed by a viscometer (SV-10, A&D Company, Limited, Japan) with detecting the driving electric current to resonate the two sensor plates at a constant frequency of 30 Hz for analysis. Surface tension of each microemulsion was determined by Tensiometer (DCAT11, Data Physics Instruments, Germany). All measurements were conducted at atmospheric pressure and a temperature of 298 K.

3.3.2 Dynamic Light Scattering (DLS)

Dynamic Light Scattering (DLS) was used for analyzing size distribution. In this work, The Zetasizer (Zetasizer Nano ZSP, MALVERN, UK) was used for measuring and size distribution of ZnSO₄ and Na₂S microemulsion as shown in **Figure 16**. This equipment was a measurement of the dispersion of light scattering by the diffusion of particles moving under Brownian motion in a static solvent. Both emulsion sample (about 5 mL) was taken from 3 experiments for determining size. The geometric mean was reported as the average droplet size. It was calculated by **Equation 4** and standard deviation were calculated using **Equation 5** then loaded it to the cuvette and measured at 25 °C for analysis.

$$\ln x_g = \frac{\sum y_i \ln x_i}{\sum y_i} \quad (4)$$

$$\ln s_g = \left[\frac{\sum n_i (\ln x_i - \ln x_g)^2}{\sum n_i} \right]^{\frac{1}{2}} \quad (5)$$



Figure 16 Zetasizer (MALVERN Zetasizer Nano ZSP)

3.3.3 Transmission electron microscopy (TEM)

Morphology of ZnS nanoparticles was performed by transmission electron microscopy (TEM). In this work, the samples were analyzed by using TEM (TEM JEM-2100, JEOL Ltd., Japan). The resulting ZnS nanoparticles were diluted in ethanol and dispersed by an ultrasonic probe of 20 minutes to uniform dispersion. ZnS nanoparticles dispersed in aqueous were poured on a carbon-coated Cu grid and waited for a solvent to be evaporated for 30 minutes at room temperature.

3.3.4 X-ray diffractometer (XRD)

XRD measurement (**Figure 17**) was carried out to analyze structures of crystals to find their crystalline phase, composition, the crystalline grain size of nanoscale materials. The resulting ZnS nanoparticles were analyzed by XRD (D8 Discover, Bruker, Germany) at a scanning rate of $1^\circ/\text{min}$ in the range of 20° to 80° . The ZnS samples were spread on the glass slide and then set in the equipment which provides an x-ray beam for the analysis.



Figure 17 XRD (BRUKER D8 DISCOVER)

3.4 Computational fluid dynamics (CFD) modeling

Computational fluid dynamics (CFD) modeling using software ANSYS FLUENT (ANSYS, Inc. USA) was simulated to describe the behavior of fluid in tank with different cavitation number. For the modeling process, the outlet velocity of the nozzle was calculated using the **Equation 2**. Incompressible Reynolds averaged Navier-Stokes equation was employed to find out the effect of velocities of microemulsion on cavitation characteristics, as follows **Equation 6** [31]. The k - ϵ turbulent model was employed to simulate the turbulent two-phase flow for a gas-liquid with spherical particles dispersion in a tank. This model estimates the turbulence kinetic energy (k) and turbulence kinetic energy dissipation rate (ϵ) by the following **Equation 2** and **8**, respectively [32, 33]. **Figure 18** shows meshed geometry of microemulsion in the tank. Smaller meshes are generated near the outlet of a multi-nozzle.

$$\rho \frac{Du}{Dt} = -\nabla \cdot P + \mu \nabla \cdot (\nabla u) + \rho F \quad (6)$$

where,

u is the fluid velocity (m s^{-1}),

ρ is the fluid density (kg m^{-3}),

P is the pressure applied to a unit volume fluid (N m^{-2}),

μ is dynamic viscosity ($\text{N m}^{-2} \text{s}$),

F is the mass force applied to a unit mass fluid (N).

$$\frac{\partial}{\partial t}(\rho k) + \nabla \cdot (\rho k u) = \nabla \cdot \left[\left(\mu + \frac{\mu_t}{\sigma_k} \right) \nabla \cdot k \right] + 2u_t E_{ij} E_{ij} - \rho \varepsilon \quad (7)$$

$$\frac{\partial}{\partial t}(\rho \varepsilon) + \nabla \cdot (\rho \varepsilon u) = \nabla \cdot \left[\left(\mu + \frac{\mu_t}{\sigma_\varepsilon} \right) \nabla \cdot \varepsilon \right] + C_{1\varepsilon} \frac{\varepsilon}{k} (2u_t E_{ij} E_{ij}) - C_{2\varepsilon} \rho \frac{\varepsilon^2}{k} \quad (8)$$

E_{ij} and μ_t are defined as **Equation 29** and **10**

$$\mu_t = \rho C_\mu \frac{k^2}{\varepsilon} \quad (9)$$

$$E_{ij} = \frac{1}{2} \left(\frac{\partial U_i}{\partial X_j} + \frac{\partial U_j}{\partial X_i} \right) \quad (10)$$

where,

μ_t is the eddy viscosity ($\text{N m}^{-2} \text{s}$),

σ_k and σ_ε are the turbulent Prandtl numbers, **วิทยาลัย**

C_μ is the turbulent model constant (0.09), **SRINAKHARIN UNIVERSITY**

$C_{1\varepsilon}$ and $C_{2\varepsilon}$ are k- ε turbulent model constant (1.44 and 1.92).

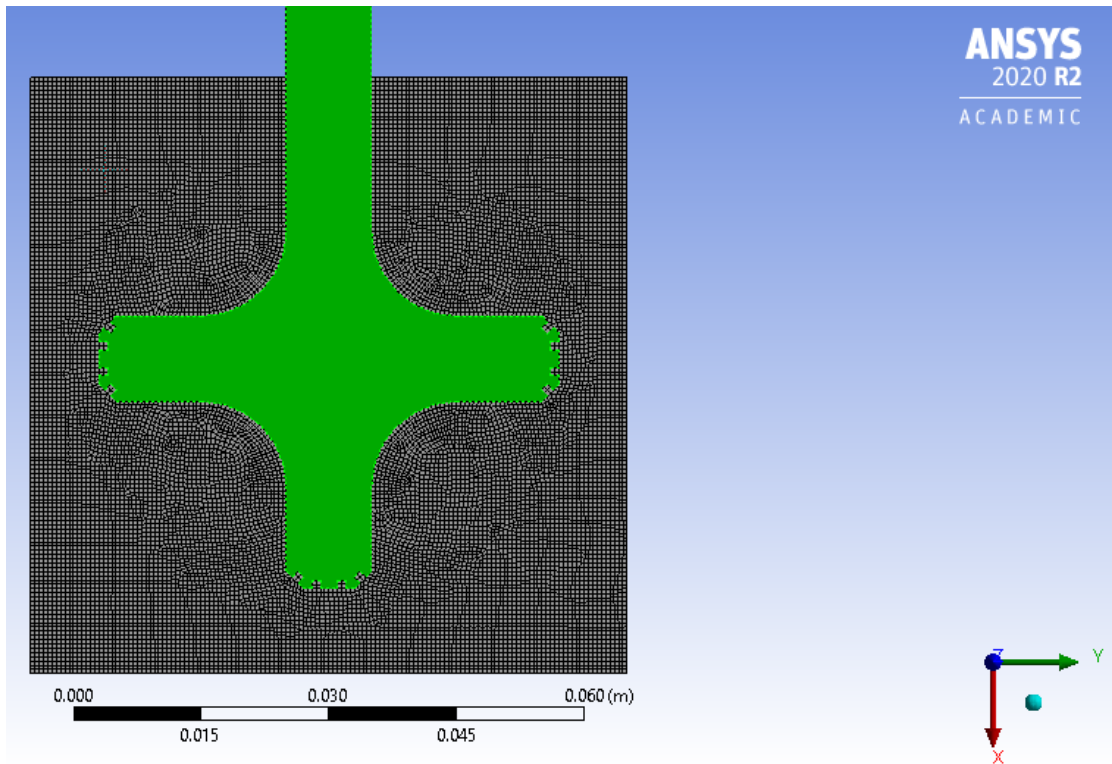


Figure 18 Meshed geometry

CHAPTER 4

RESULTS AND DISCUSSION

This research focused on synthesis of ZnS nanoparticles by the microemulsion technique enhanced by hydrodynamic cavitation. Influence of number of passages, cavitation number (C_v) and water to surfactant molar ratio (W_0) on microemulsion characteristics was experimentally investigated at cavitation number of 1.8, 3.2, and 7.1 and water to surfactant molar ratio of 7, 11, and 15. Change of turbulence intensity in system and rheological properties of suspension would affect the collision of microemulsion which in turn affects formation of ZnS within the confined volume of each microemulsion. The rheological properties and size distribution of microemulsion were characterized by various techniques including viscometer, tensiometer and dynamic light scattering. Also, simulation model of microemulsion behavior was employed to explore the effect of the cavitation number on velocity distribution and turbulent dissipation energy within the experimental vessel. Then, ZnSO₄ and Na₂S microemulsions were mixed for ZnS synthesis. Characteristics of ZnS nanoparticles samples were investigated. TEM and XRD analyses were conducted to identify the size distribution, morphology, and crystalline structure.

4.1 Characteristic of relevant substances

This part aims to systematically introduce rheological properties of suspension of microemulsions, which were recognized as a water-in-oil system. The nature of reactant aqueous solution and the influence of the water to surfactant molar ratio on rheological properties of microemulsion were studied. The analyses of initial substances would help to understand their rheological properties and explain their effects on the changes of the size distribution of microemulsion.

Solubility of ZnSO₄ and Na₂S in aqueous solution is an important parameter to obtain a homogeneous mixture for microemulsion without any undissolved matter. The ZnSO₄ and Na₂S aqueous solutions were prepared using 28.8 g and 24.0 g per 1 dm³ of water to achieve concentration of 0.1 molar. The data on the reactant solubility correlated with temperature were reported by Saha et al. It has been shown that the solubility of ZnSO₄ in water is 600 g/ dm³ while the solubility of Na₂S in water is 288

g/dm^3 at 35 °C [34]. Thus, amount of reactant of 0.1 mole could be completely soluble in water of 1 dm^3 . ZnSO_4 could easily ionized to Zn^{2+} and SO_4^{2-} at room temperature and Zn^{2+} might easily react with highly active S^{2-} ions produced from Na_2S [35]. Moreover, ZnSO_4 and Na_2S droplets are mixed which results in the interchange of reactants between Zn^{2+} and S^{2-} species. It would lead to formation of ZnS nanoparticles. Murcia et al reported the solubility of ZnS in an aqueous solution is $4.8 \times 10^{-5} \text{ g/dm}^3$ in the temperature range 200-300 °C due to the electronegativity difference between cations and anions is low resulting in strong ionic bonding. [36].

The rheological properties of ZnSO_4 microemulsion were also investigated. Data on density, viscosity and surface tension of ZnSO_4 microemulsion are shown in **Figure 19**. Experimental data has revealed that relevant substances exhibit considerable changes in rheological properties when adding a certain amount of water into the system. As a continuous phase or water to surfactant molar ratio (W_0) of 0, a mixture of cyclohexane, Triton X-100 and n-hexanol exhibited density, viscosity and surface tension of 840.6 kg/m^3 , 0.0014 kg/m s and $25.5 \times 10^{-3} \text{ N/m}$, respectively. After addition of ZnSO_4 in water to the mixture with designated water to surfactant molar ratio (W_0) of 7, 11 and 15, the changes in density, viscosity and surface tension were observed as shown in **Figure 19**. It could be confirmed that the density, viscosity and surface tension of ZnSO_4 microemulsion increased with an increase in water content, namely W_0 . These results were in a good agreement with that of Pan et al. reported that increasing W_0 would result in reduced effectiveness of surfactant which could indicate a reduction in the stability of the emulsion [37]. Also, Faris et al. reported a relationship between viscosity and surface tension. An increase in viscosity would enhance the attraction forces and intermolecular strength of cohesion. Thus, the surface tension of the solutions also increases [38].

Analyses of these rheological properties show that the stability and fluidity of microemulsion depend on the water to surfactant molar ratio. The properties of such emulsions are also very important to the formation and size distribution of microemulsion for ZnS nanoparticles synthesis.

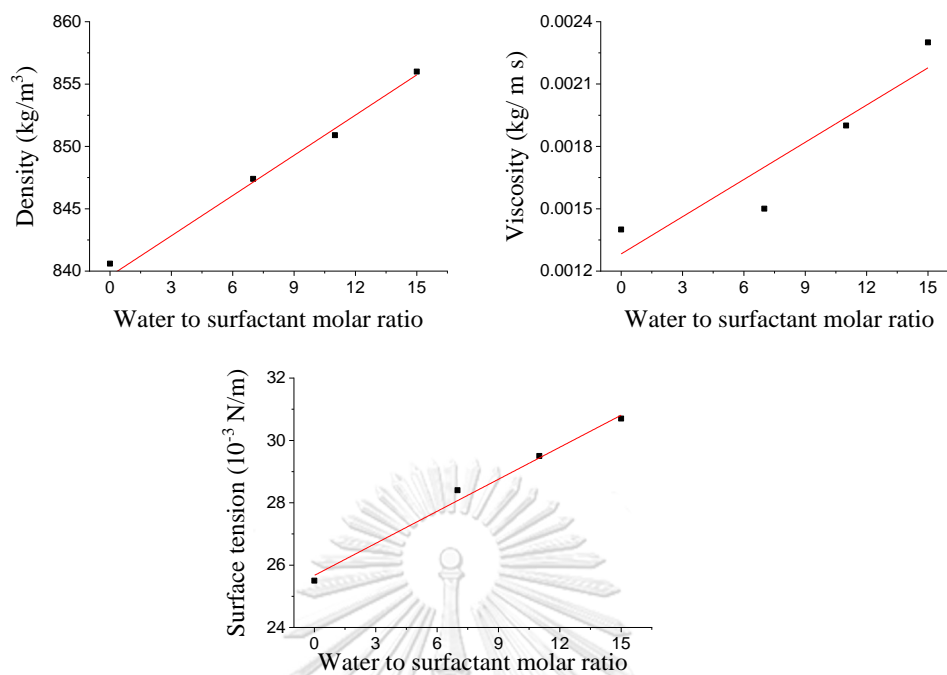


Figure 19 Rheological properties of ZnSO_4 microemulsion prepared with different W_0

4.2 Investigation of properties and size distribution of microemulsion prepared by hydrodynamic cavitation

In this work, hydrodynamic cavitation (HC) was used for microemulsion preparation in prior to ZnS nanoparticles synthesis. Cavity in microemulsion by HC can be generated from flowing microemulsion as it passes through a constriction in a multi-nozzle. At the constriction, the kinetic energy of the microemulsion increases and pressure falls below the vapor pressure, generating cavities. A downstream of the constriction, the velocity of the fluid reduces resulting in the implosion of the cavities and very high-intensity fluid turbulence is also generated. It acts as a main driving force for the formation of the microemulsion.

4.2.1 Effect of number of passages on size distribution of microemulsion

The number of passages of 300, 600, 900, 1,200 and 1,500 was varied for evaluating its effect on size distribution of ZnSO_4 and Na_2S microemulsion. It could be related to energy dissipation in the system. The cavitation number and water to surfactant molar ratio were kept constant at 1.8 and 7, respectively.

Figure 20 reveals a change in number of passages according to variation of circulation time. It is clearly seen that the size of the microemulsion was dependent on the number of passages. As the number of passages increases from 300 to 600 at C_v of 1.8, the size distribution of both $ZnSO_4$ and Na_2S microemulsions became narrower and shifted towards smaller diameters. A distinct decline in average size of both microemulsions could be observed when number of passages was increased from 300 to 900 as shown on **Table 1**. However, a further increase in the number of passages from 1,200 to 1,500 resulted in a slight decline in the average size. Similarly, Carpenter et al. and Zhang et al. reported that an increase in the number of passages could result in a decrease in the average size of droplets before achieving a constant value [6, 8]. Also, Das et al suggested that the energy dissipation in the system depended on the number of passages or circulation time as could be determined by **Equation 11** [39]. It can be explained by the dispersion of aqueous phase in cyclohexane (continuous oil phase) would require high energy to break the oil-water interface. The experimental result in **Figure 20** reveals that the amount of dissipated energy was proportional to the number of passages. In this work, the highest value of the dissipated energy was achieved at the condition of 1,500 passages. It can be explained in terms of the increased energy imparted to the drops which enhanced the mixing of immiscible phases, thus resulting in a higher breakage frequency and reduced in the average size of the microemulsion [40].

$$E = P \times V \times t \quad (11)$$

where,

E is energy dissipation in system (J)

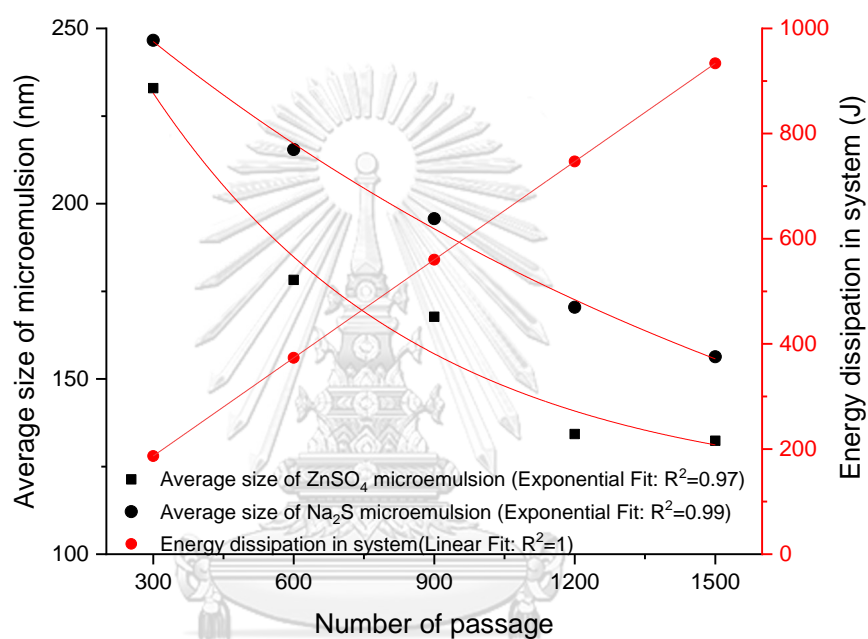
P is pressure drop across a multi nozzle ($N\ m^{-2}$)

V is volumetric flow rate ($m^3\ s^{-1}$)

t is circulation time (s)

Table 1 Average size and standard deviation of ZnSO₄ and Na₂S microemulsion

Number of passages	300	600	900	1,200	1,500
ZnSO ₄	232.9± 1.7	178.2± 1.2	167.7± 1.2	134.3± 1.2	132.2± 1.2
Na ₂ S	246.6± 1.5	215.4± 1.2	195.7± 1.2	170.4± 1.1	156.3± 1.1

**Figure 20** Energy dissipated into the system and average size of ZnSO₄ microemulsion

4.2.2 Effect of cavitation number on size distribution of microemulsion

Cavitation number is an important factor in determining the efficiency of hydrodynamic cavitation as it affects turbulence intensity. In this part, the cavitation number was varied from 1.8 to 3.2 and 7.1 by changing the velocity from 10.6 to 8.0 and 5.3 m/s, respectively. The behavior of microemulsion leading to different size distribution at various C_v was investigated using modelling by computational fluid dynamics. $ZnSO_4$ and Na_2S microemulsion were prepared with the molar ratio of water to surfactant of 7.

The simulation results show velocity and turbulence kinetic energy contours for microemulsion in tank at C_v of 1.8 to 3.2 and 7.1 as shown in **Figure 21**. It can be seen that a multi-nozzle produced an outward fluid flow from the center towards the walls where the flow was split into 3 directions. The right and left multi-nozzle thrust the microemulsion to the wall vertically, while the bottom multi-nozzle formed an axial fluid stream to the base of the tank. The velocity of the microemulsion is very high near the outlet zones of the multi-nozzle zones and base wall at higher C_v . In the case of lower C_v or higher Re , the velocity contours are significantly high and a broad magnitude which is in agreement with the kinetic energy contours.

Figure 21 demonstrates the turbulence kinetic energy of the microemulsion at C_v of 1.8 to 3.2 and 7.1. The turbulence kinetic energy was increased with a decrease in C_v . Moreover, the turbulent kinetic energy dissipation is higher near the outlet zones of the multi-nozzle, which is in agreement with the velocity contour. Along with higher Re , a large turbulence intensity was produced and caused a uniform dispersion of energy over the tank. Pukkella et al. suggested that a higher turbulent energy dissipation rate could help to improve the effectiveness of circulation and reduce the size of the microemulsion [41].

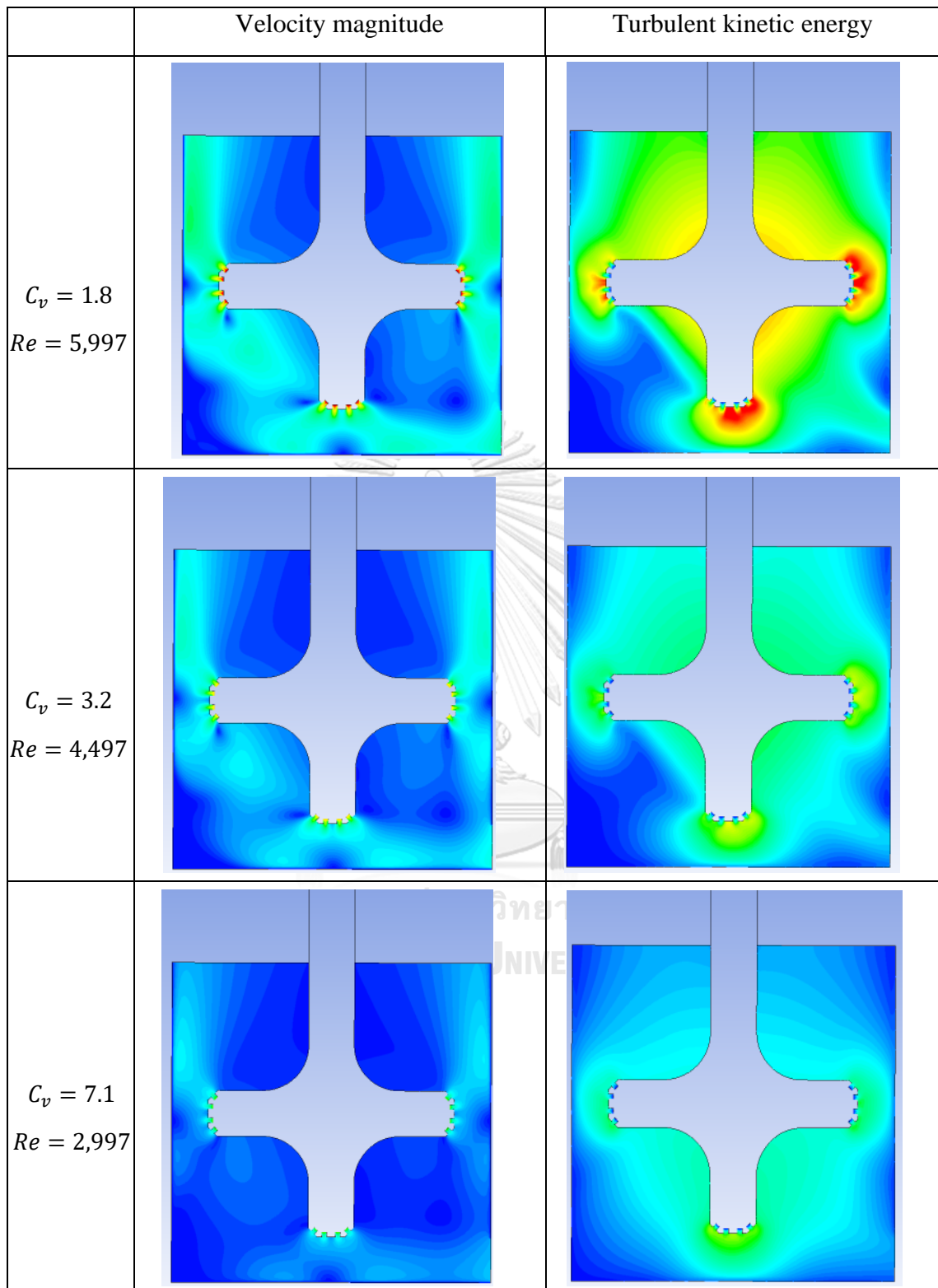


Figure 21 Contour of velocity magnitude (m s^{-1}) and turbulent kinetic energy ($\text{m}^2 \text{s}^{-2}$) at different C_v

Figure 22, 23 (a) and (b) reveal size distribution and average size of ZnSO_4 and Na_2S microemulsion with differences in the number of passages were increased with an increase in C_v . At lower C_v or higher Re , the size distribution and average size of microemulsion were decreased. An increase in velocity pass through the nozzle induces stronger turbulence kinetic energy which led to more turbulence and shear and generates more vapor cavities. Higher cavitation intensity is responsible for the significant reduction in mean droplet diameter as energy density increases [8, 40, 42, 43]. The turbulence kinetic energy dispersion was higher near a multi-nozzle as seen in **Figure 21**, which could produce a high turbulence intensity relative to the others. These results were in good agreement with that of Sarkar et al. suggesting that the increase in the turbulent energy dissipation rate would provide more shearing action [44]. Hence, smaller reverse micelles exist near the multi-nozzle region while larger reverse micelles appear in farther regions. Fathi Roudsari et al reported that the higher velocity magnitude led to increasing in turbulent kinetic energy throughout the tank which resulted in improved recirculation rate and breakage rate [40]. Other studies, where hydrodynamic cavitation was used for microemulsion preparation, reported that the cavitation number and number of passages are the important parameters that affect the cavitating condition inside the cavitating device. An increase in the number of passages and velocity passes through the nozzle induces high-intensity fluid turbulence which causes the disruption of larger droplets into smaller ones [6, 8, 19].

Simulation results pointed that the contour of velocity and turbulence kinetic energy were affected by cavitation number. Increasing cavitation number was found to be effective in the circulation of microemulsion throughout the inner region of the tank leading to reducing the microemulsion size.

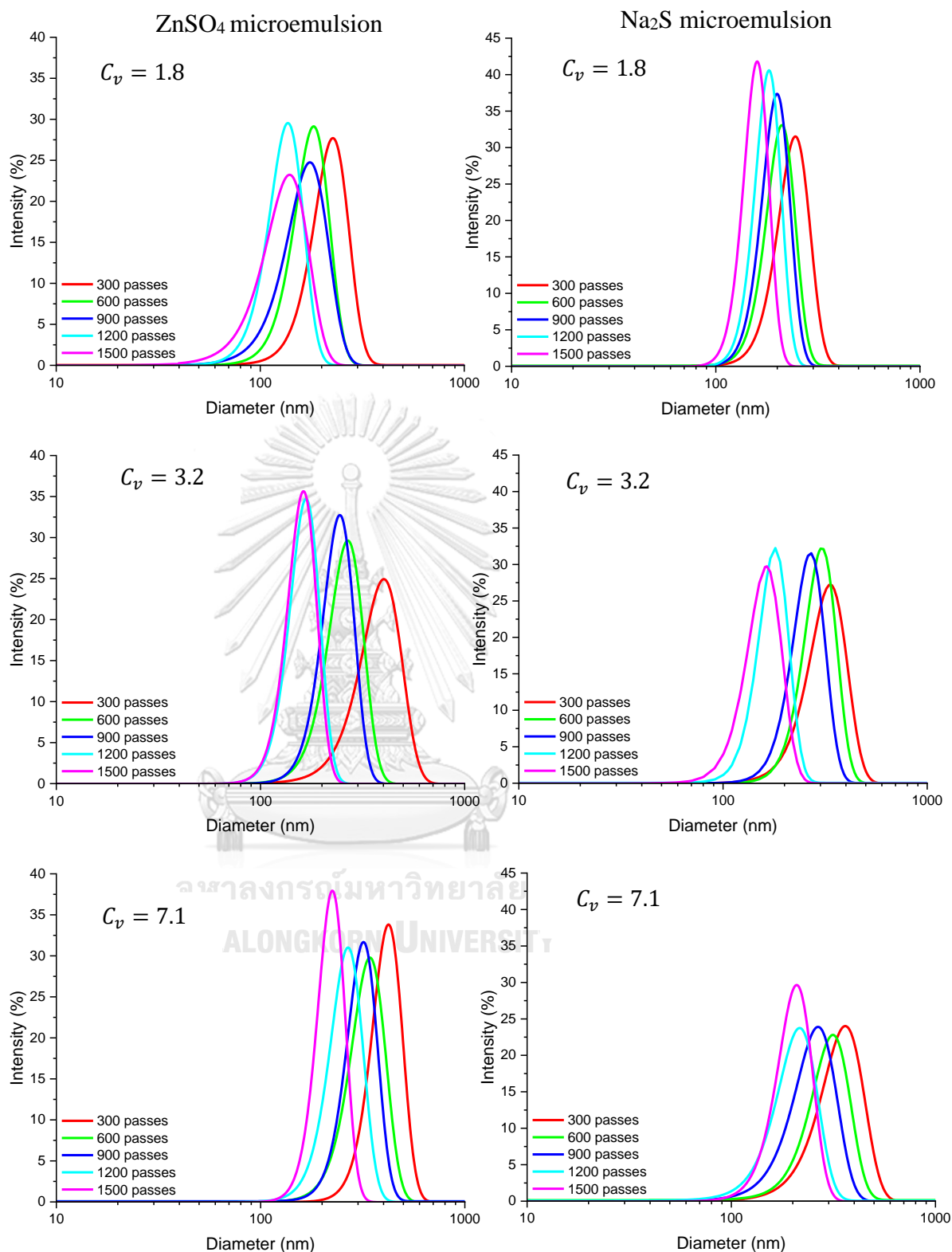


Figure 22 Effect of C_v on size distribution of microemulsions with a difference in the number of passages

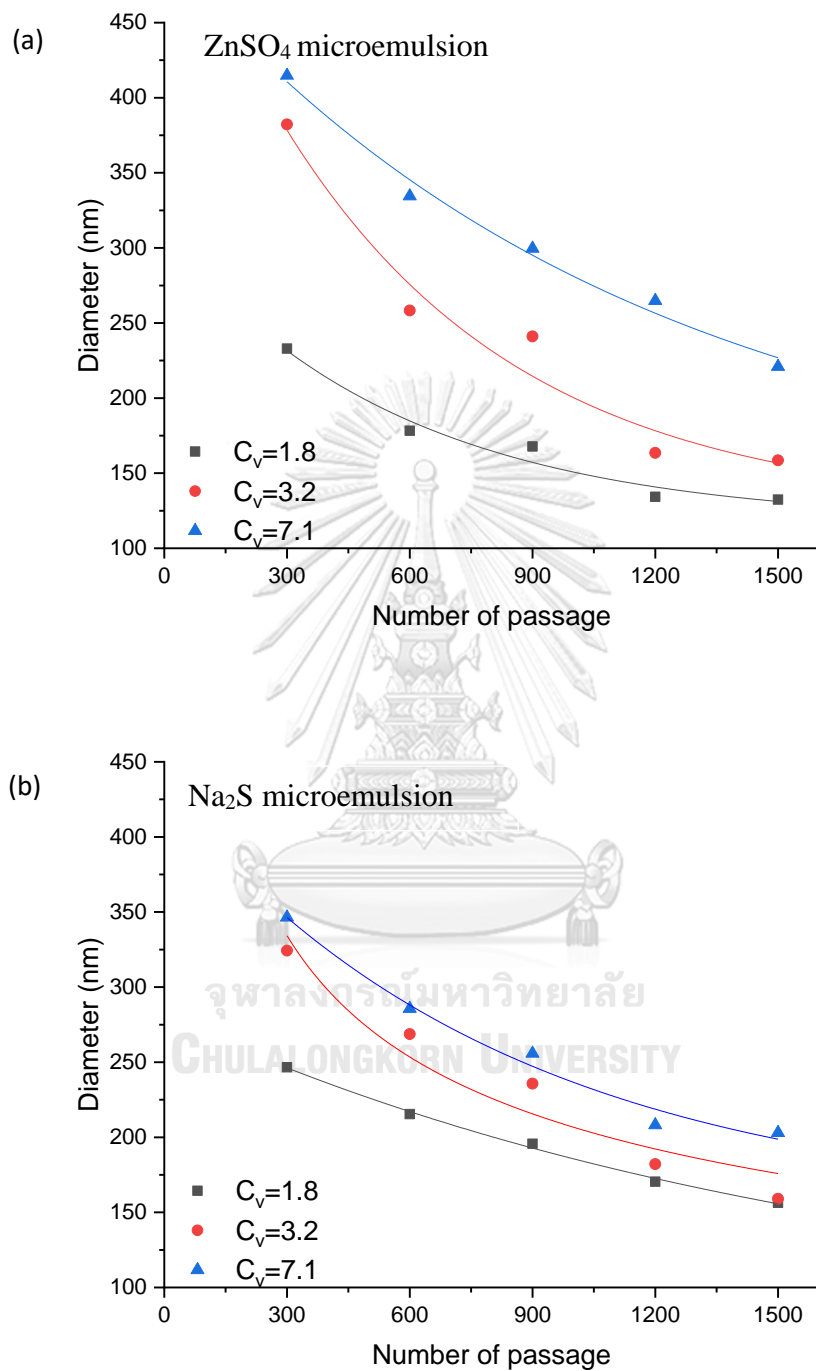


Figure 23 Average size of microemulsion with difference in C_v of (a) ZnSO₄ microemulsion and (b) Na₂S microemulsion

4.2.3 Effect of water to surfactant molar ratio on size distribution of microemulsion

The water to surfactant molar ratio (W_0) of 7, 11 and 15 was employed for preparing microemulsion of $ZnSO_4$ and Na_2S aqueous solution with a designated cavitation number (C_v) of 1.8. The influence of water to surfactant molar ratio (W_0) on rheological properties and size distribution of microemulsion was experimentally investigated in 4.1 and replotted with Re as shown in **Figure 24**. The different rheological properties would affect the collision of microemulsions, and this ultimately defines the size distribution of microemulsion.

The rheological properties are significantly different on increasing water to surfactant molar ratio, indicating water to surfactant molar ratio has a major effect on the density, viscosity and surface tension of $ZnSO_4$ microemulsion. Increasing density and viscosity in turn affect the mobility of the microemulsion which is caused by the polarity of water molecules inside. It would lead to the improvement of the fluidity of the microemulsion. The ability to control the rheological properties and flowability of the microemulsion would be enhanced by increasing the water content (W_0) [45]. Farah et al. and Tatar et al. also reported that an increase in the water content resulted in an increase in surface tension of oil-water interface [46, 47]. Moreover, Reynolds' number of the circulated microemulsion was oppositely hindered with the increase in the water content as could also be observed in **Figure 24**.

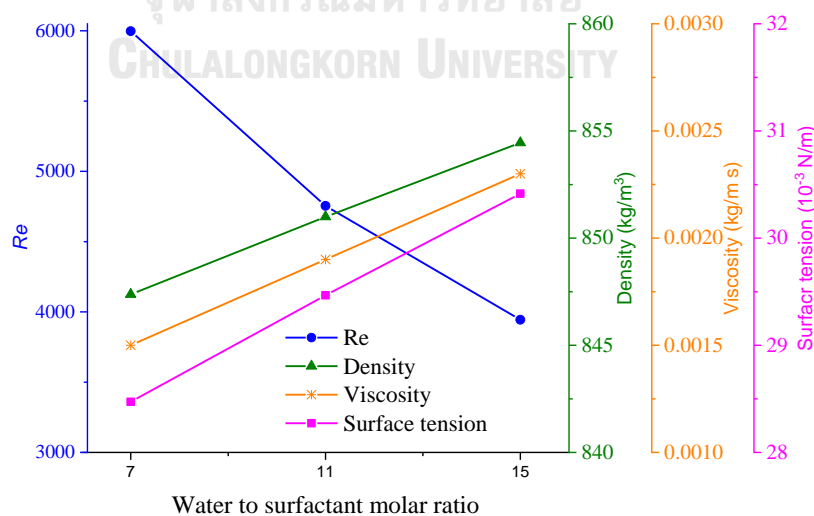


Figure 24 Rheological properties and Re of $ZnSO_4$ microemulsion prepared with different W_0

Apart from the changes in rheological properties, the difference in average size and size distribution of microemulsion together with various W_0 value are also examined. As summarized in **Figure 25, 26 (a) and (b)**, the size distribution of microemulsion is correlated with water to surfactant molar ratio. The increasing W_0 led to an increasing of average size and size distribution of microemulsion. When the W_0 increases from 7 to 15 of 1,500 passages, the average size of $ZnSO_4$ microemulsion increases from 132.2 ± 1.1 to 173.5 ± 1.2 nm, while the average size of Na_2S microemulsion increase from 156.3 ± 1.1 to 177.1 ± 1.2 nm. The water content in the system can be also raised by also increasing surfactant molar at constant W_0 levels. The surfactant functions by reducing the surface tension of the water by adsorption at the oil and water due to the adsorbing effect at the liquid-liquid interphase. The adding water content to the system led to increased surface tension of oil-water, Meanwhile, Takahashi et al. reported that the minimum energy (ΔF) required for microemulsion formation depends on surface tension as given below in **Equation 12** Error! Reference source not found. [10, 48]. Decreasing the water/oil interfacial tension lessens the energy for microemulsion formation. Accordingly, in case of low water content, the average size of both microemulsions were smaller and uniform in shape. Mandato et al. revealed that the diameter of the droplet depends on the surface tension of both liquids. An increase in liquid surface tension could hinder liquid disintegration, resulting in an increase in the amount of energy required for formation, as well as an increase in droplet diameter [49]. In addition, Ithnin et al. and Sartomo et al. reported that the water ratio also affects viscosity of microemulsion. Increasing the water content resulted in a significant increase in viscosity of microemulsion. Increasing in tension and viscosity of solution lessen the flow fluid velocity and the kinetics of formation thus increase size of microemulsion [42, 50]. Furthermore, control of size distribution of microemulsion would affect formation of ZnS nanoparticles precipitating within the confined volume of microemulsion as suggested by Charinpanitkul et al. [51]. Therefore, the size distribution of microemulsion was a result of several simultaneous events. Based on these results, it could be confirmed that the water to surfactant molar ratio is one of the parameters

associated with the formation of microemulsion which could affect the size distribution of microemulsion.

$$\Delta F = \frac{16\pi\gamma^3}{3(P_{sat}-P_o)^2} \quad (12)$$

where,

ΔF is the minimum energy (erg),

γ is the surface tension of the liquid (mN/m),

P_{sat} is the saturation pressure (dyne/cm²),

P_o is the atmospheric pressure (dyne/cm²).



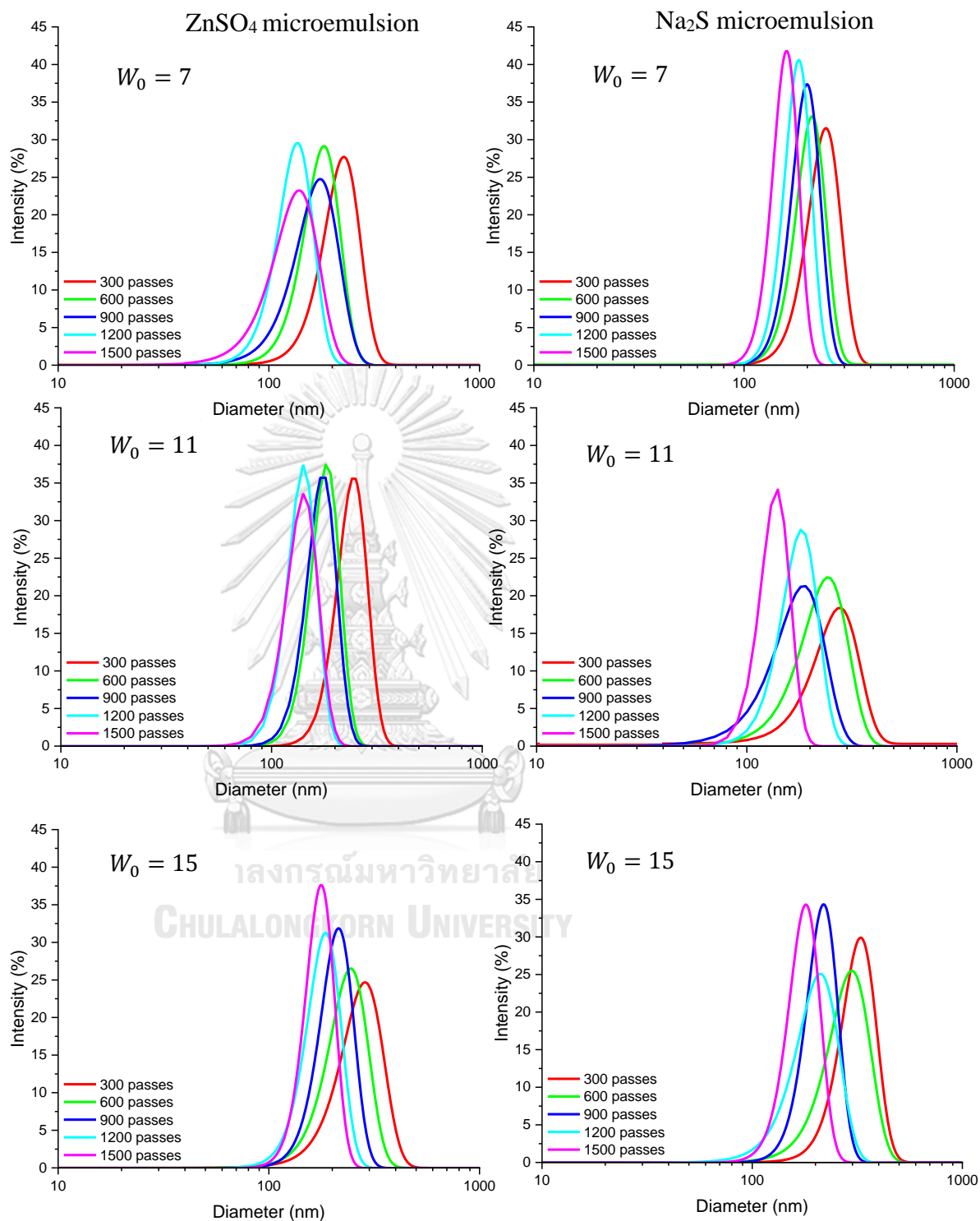


Figure 25 Effect of water to surfactant molar ratio on size distribution of microemulsion with difference in number of passages

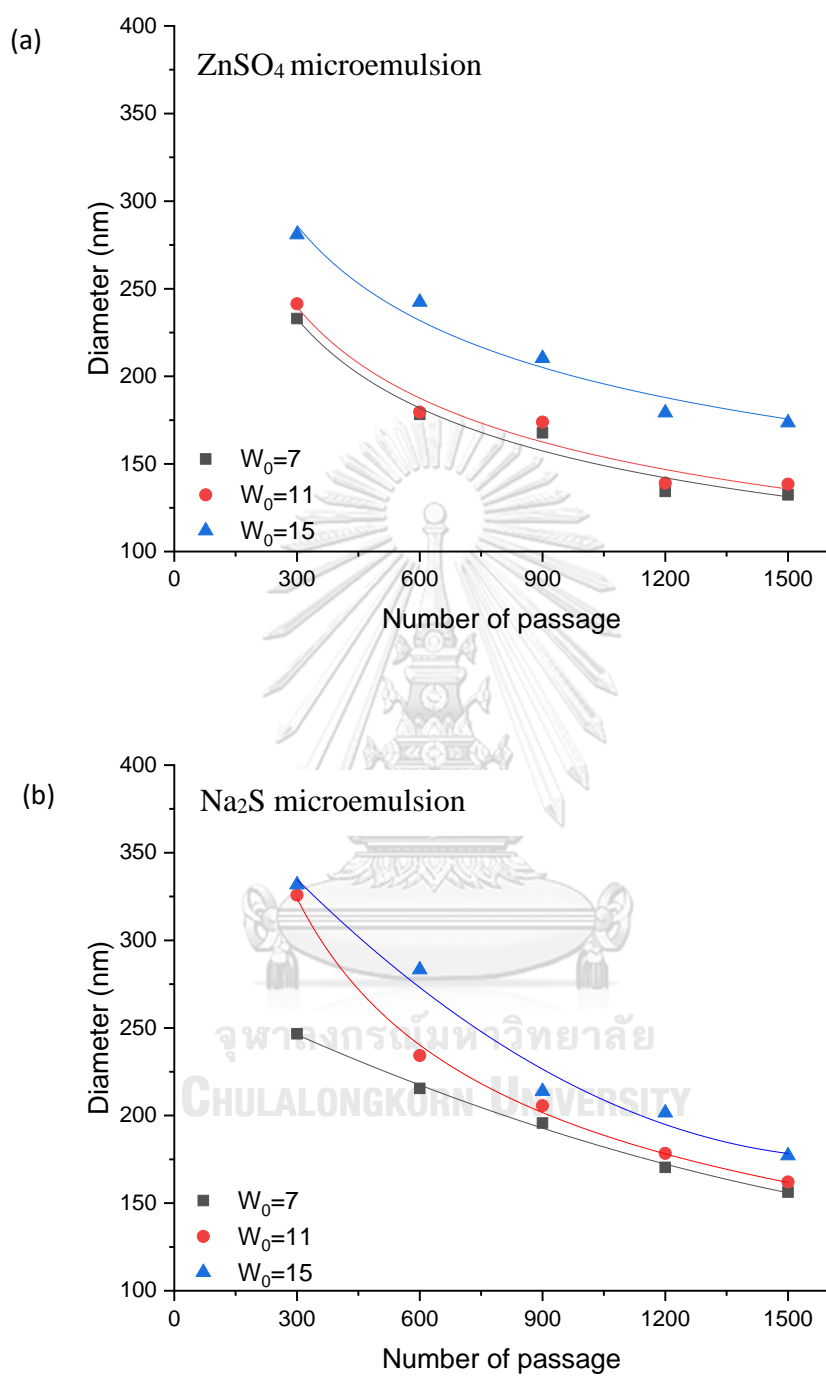


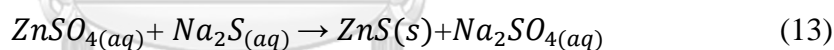
Figure 26 Average size of microemulsion with difference in W_0 (a) ZnSO₄ microemulsion and (b) Na₂S microemulsion

4.3 Investigation of size distribution and morphologies of ZnS nanoparticles synthesized by microemulsion

The synthesis of ZnS nanoparticles by microemulsion method is a bottom-up approach. ZnSO₄ microemulsion and Na₂S microemulsion were mixed under the hydrodynamic cavitation for enhancing their interaction, which would in turn affect formation of ZnS nanoparticles. During this process, the chemical reaction takes place inside the confined volume of each microemulsion. ZnSO₄ and Na₂S droplets are mixed by circulating and the droplets continuously collide which results in the interchange of reactants between Zn²⁺ and S²⁻ species. It would lead to nucleation and growth of ZnS nanoparticles. Meanwhile, the surfactant layer on the outer surface of each microemulsion would help prevent the resultant ZnS nanoparticles from aggregation [4, 52]

4.3.1 Yield of synthesized ZnS nanoparticles

Chemical reaction of ZnS is a precipitation reaction which is irreversible. The precipitation reaction of ZnS is shown in **Equation 13** Error! Reference source not found.. Yields by weight of synthesized products could be calculated by **Equation 14**. Error! Reference source not found.



$$\text{Percent yield} = \frac{\text{actual yield}}{\text{theoretical yield}} \times 100 \quad (14)$$

where,

Actual yield is the amount of product obtained from experiment

Theoretical yield is the amount of product obtained from stoichiometry

Yields by weight of synthesized product at various W₀ (7, 11 and 15) with different C_v were shown in **Figure 27**. When focusing on the effect of C_v, at W₀ of 7, product yields were 90.3%, 87.1%, and 82.4% with respect to C_v of 1.8, 3.2, and 7.1, respectively as shown in **Figure 27 (a)**, respectively. The different stages of nanoparticle formation process inside water droplets can be explained as: chemical reaction, nucleation and particle growth. The first stage is the chemical reaction between the two reactants. During this process, when droplets with either one of the

reactants are mixed by constant circulating and the droplets continuously collide which results in the interchange of reactants and then these S^{2-} ions react with Zn^{2+} ions to form the ZnS monomers. The second stage in nanoparticle synthesis is nucleation because of crystal formation. In this stage, atoms and molecules rearrange to create seeds or nuclei in microemulsion, hence the concentration of monomer in solution decreased. The third stage of nanoparticle formation is called the growth of nanoparticles. Almost all the monomers in solution are used to grow existing nanocrystals. when a crystal has reached a critical size [3].

The reaction of ZnS synthesis is ionic reaction which very fast reaction kinetics. Rauscher et al. demonstrated a time analysis of $CaCO_3$ precipitation in a typical microemulsion system. the typical time constants for the chemical reaction, nucleation, and particle growth were 10^{-12} – 10^{-8} , 10^{-12} – 10^{-8} and 10^{-3} – 10^{-1} s, respectively [53]. Thus, the product molecules are instantaneously formed during circulation. Rajoriya et al. reported that higher velocity through the cavitating device maximizes the intensity of turbulence and generated a greater number of cavities [39, 54]. It could help to improve frequency of collision and reaction between droplets result in a higher reaction rate and leading to higher production yield. At higher C_v , circulation is not complete resulting in inhomogeneities of the spatial concentration distribution. Thus, motion and collision exchange are low leading to lower production yield.

When focusing on the effect of W_0 , at C_v of 1.8, product yields were 90.3%, 92.8%, and 95.5% for W_0 of 7, 11, and 15, respectively as shown in **Figure 27 (b)**. Roman et al. reported the mass production in the precipitation reactions is equal to the mass dissolved in the aqueous phase [55]. Moreover, the yield increases as the water fraction in the liquid increases. Pileni et al. suggested when decreasing W_0 , Rigidity of reverse micelles interface was higher, lowering intermicellar exchange and reaction rates resulting in decreasing in product yields [56].

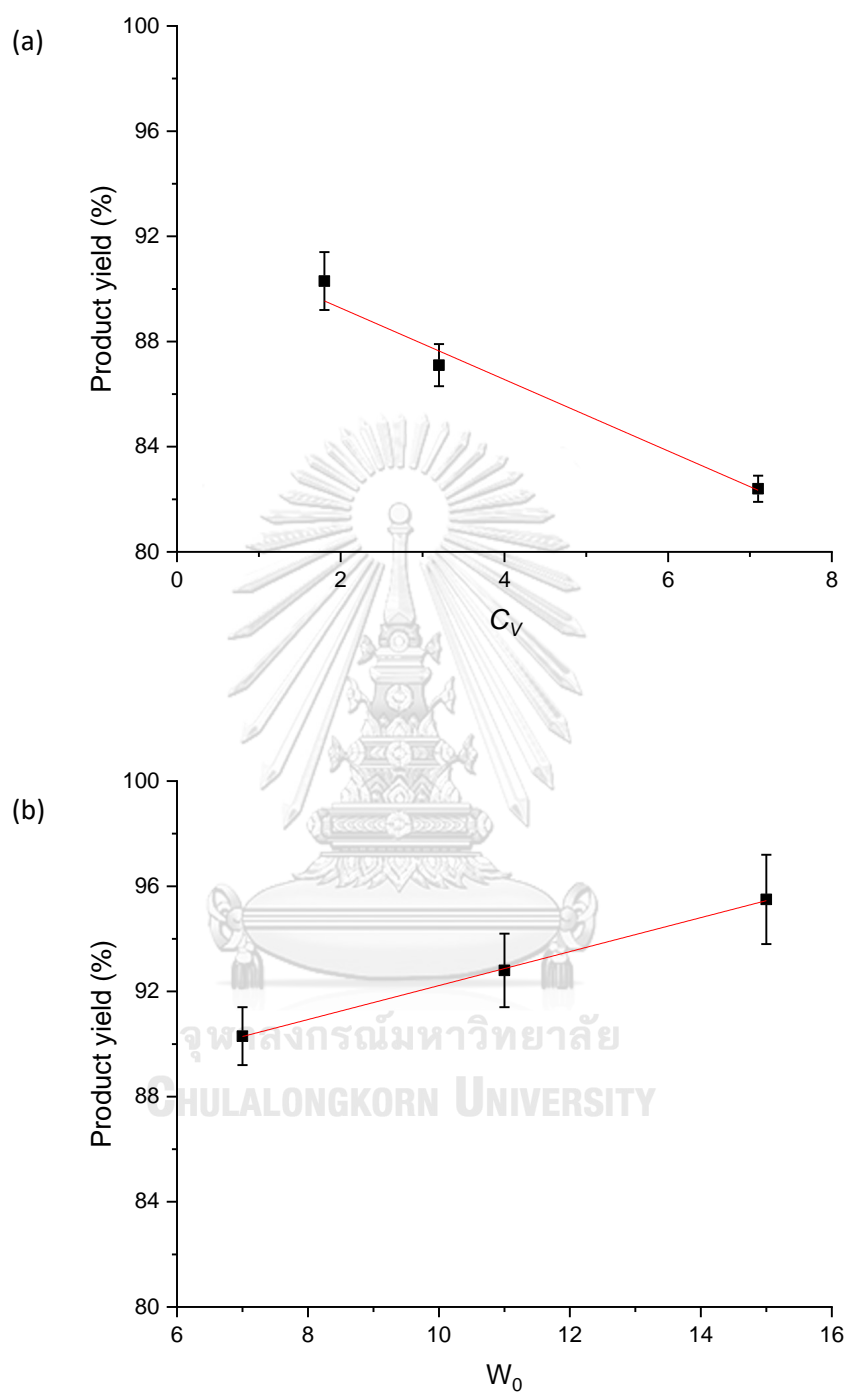


Figure 27 Yields of weight of synthesized product at: **(a)** various C_v and **(b)** various W_0

4.3.2 Morphologies and size distribution of ZnS nanoparticles

The morphologies of the as-prepared nanoparticles were studied by HRTEM and the images are depicted in **Figure 28**. Additionally, image processing software (ImageJ) was also applied to HRTEM images to analyze size distribution of ZnS. Apparently, all ZnS nanoparticles possess spherical morphology with clusters due to agglomeration of the nanosized particles. The very small crystallites are visible at higher magnification. The typical size distribution of ZnS nanoparticles obeys the Gaussian model within a range below 10 nm which indicates the formation of ZnS quantum dots. The results exhibit the significant changes in the size distribution of the synthesized ZnS nanoparticles when varying microemulsion parameters. The average size increases, and particle size distribution are broader when cavitation number and water to surfactant molar ratio increase. The average size of the resultant ZnS nanoparticles prepared with W_0 of 7, 9, and 11 increased from 4.6 ± 0.7 to 5.4 ± 1.1 and 6.1 ± 1.3 nm as shown in **Figure 28 (a)-(c)**, respectively. This result also further confirmed the change of diameters of the resulting samples, in agreement with the size distribution of microemulsion in the previous section. This should be noted that the size of the microemulsion should be extremely small to obtain well-defined shapes with a narrow distribution of the nanoparticles. In the templates of larger diameters ($C_v = 3.2$ and 7.1), excessive growth of the resultant nanoparticles particles could be observed in **Figure 28 (d) and (e)**.

This result agrees with results obtained by Vaidya S. et al. These authors reported an important influence of the molar ratio of water to surfactant on the size distribution of nanoparticles [25]. This can explain that the change in the size of ZnS nanoparticles varied with different W_0 which attribute to the difference in reverse micelle size. Li et al and Barman and Sarma. reported that mass transfer rate could be affected by surfactant rigidity at the interface resulting in the formation of nanoparticle products with different size distributions [1, 57]. A low W_0 provided lower content of water in microemulsion system, hence a small size of ZnS products is formed. After a small micelle of $ZnSO_4$ reactant interacts with a small micelle of Na_2S reactant, the reactants mass transfers occur to each other and form the ZnS particle in each small micelle. In contrast, with A higher W_0 , this reaction is severe and leads to the rapid formation and aggregation of primary nuclei due to the

enhancement of exchange rate for the reactants. It was assumed that these reverse micelles could be used as templates to control the final size and shape of the particles. [23, 58, 59].

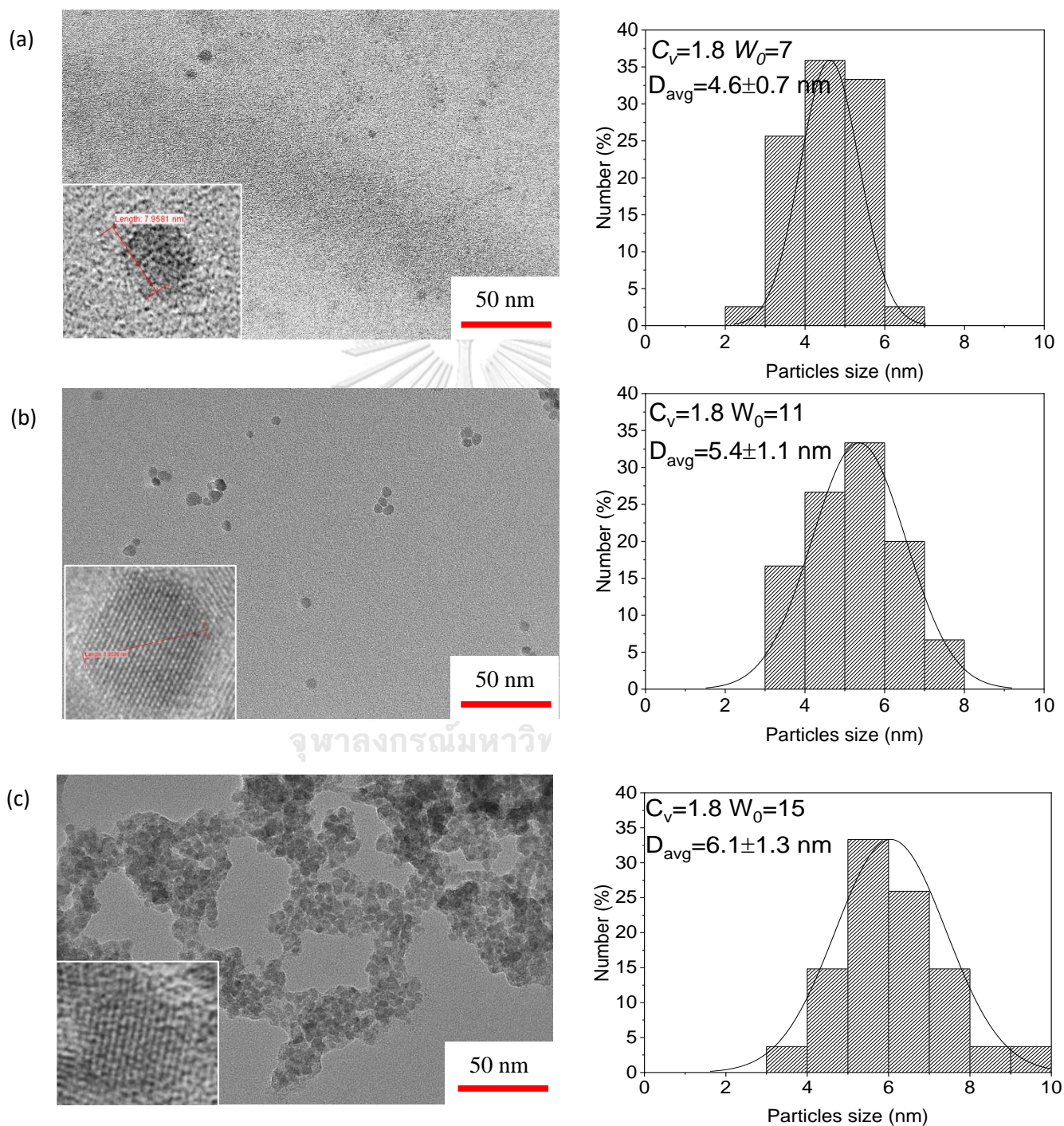


Figure 28 TEM micrograph and size distribution of ZnS nanoparticles

(a) $C_v=1.8$, $W_0=7$, (b) $C_v=1.8$, $W_0=11$ and (c) $C_v=1.8$, $W_0=15$

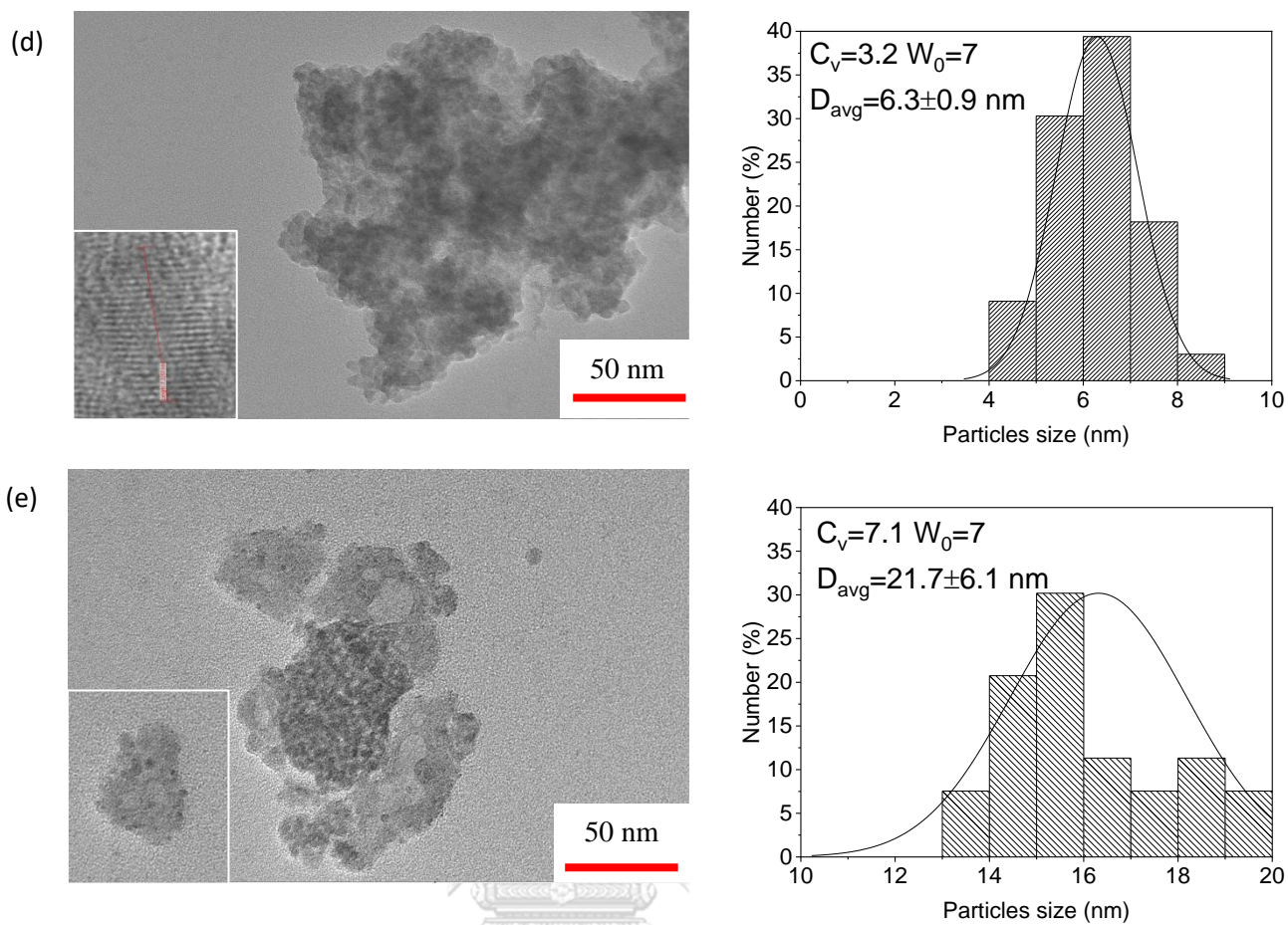


Figure 25 TEM micrograph and size distribution of ZnS nanoparticles

(d) $C_v=3.2$, $W_0=7$ and (e) $C_v=7.7$, $W_0=7$ (continuous)

4.3.3 Crystalline structure of ZnS nanoparticles

To identify structure of as-synthesized ZnS nanoparticles products, a typical X-ray diffraction technique was conducted to demonstrate that these products were ZnS. **Figure 29** presents the XRD patterns of the as-synthesized ZnS. The diffraction peaks appearing at 28.9 °, 48.3 °, 57.4 ° would correspond to (111), (220) and (311) planes representing the cubic crystalline structure without any impurity [JCPDS card no. 5–566]. However, all samples possess diffraction peak with different shape and intensity, revealing the difference in crystalline size of ZnS product [60]. The crystalline domain size was calculated using Debye–Scherrer diffraction formula (**Equation 15**). XRD patterns also indicate that the peaks are gradually weaker and broader with decrease in the molar ratio of water to surfactant, suggesting that the crystalline size become smaller. The crystallite size of ZnS nanoparticles synthesized with W_0 of 7, 11 and 15 were 4.4, 4.6, and 5.1 nm, respectively as shown in **Table 2**. Khiew et al. and Liu et al. suggest that increasing the molar ratio of water to surfactant would favor the formation of ZnS phase [58, 61]. Meanwhile, all values of crystallite size are similar and very small for varying in cavitation number. This could be due to the low number of atoms derived from low amount of reactants, which diminishes the probability of crystallites agglomeration and helps to restrict the particle size.

$$D_c = \frac{K\lambda}{\beta \cos\theta} \quad (15)$$

where,

$K = 0.9$ for shape factor of ZnS cubic structure

$\lambda = 1.5405 \text{ \AA}$ is the X-ray wavelength

β is the full width at the half maximum of the diffraction peak (radians)

θ is the diffraction angle (radians)

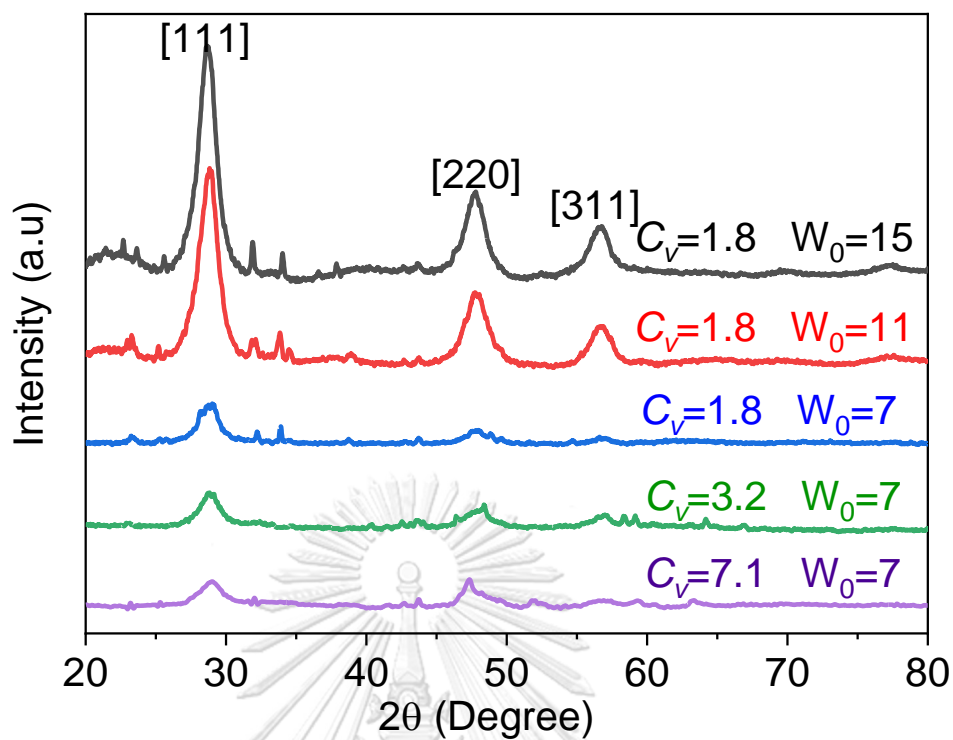


Figure 29 XRD patterns of ZnS nanoparticles

Table 2 The crystalline size of ZnS nanoparticles

C_v	W_0	Crystalline size (nm)
1.8	15	5.1
	11	4.6
	7	4.4
3.2	7	3.9
7.1	7	3.7

In addition, Selected area electron diffraction (SAED) was used to determine the microcrystalline structure of ZnS nanoparticles. The HRTEM image and the corresponding SAED pattern (as shown in **Figure 30**) of ZnS nanoparticles at C_v of 1.8 and W_0 of 15 clearly indicate the polycrystalline structure of ZnS product [62].

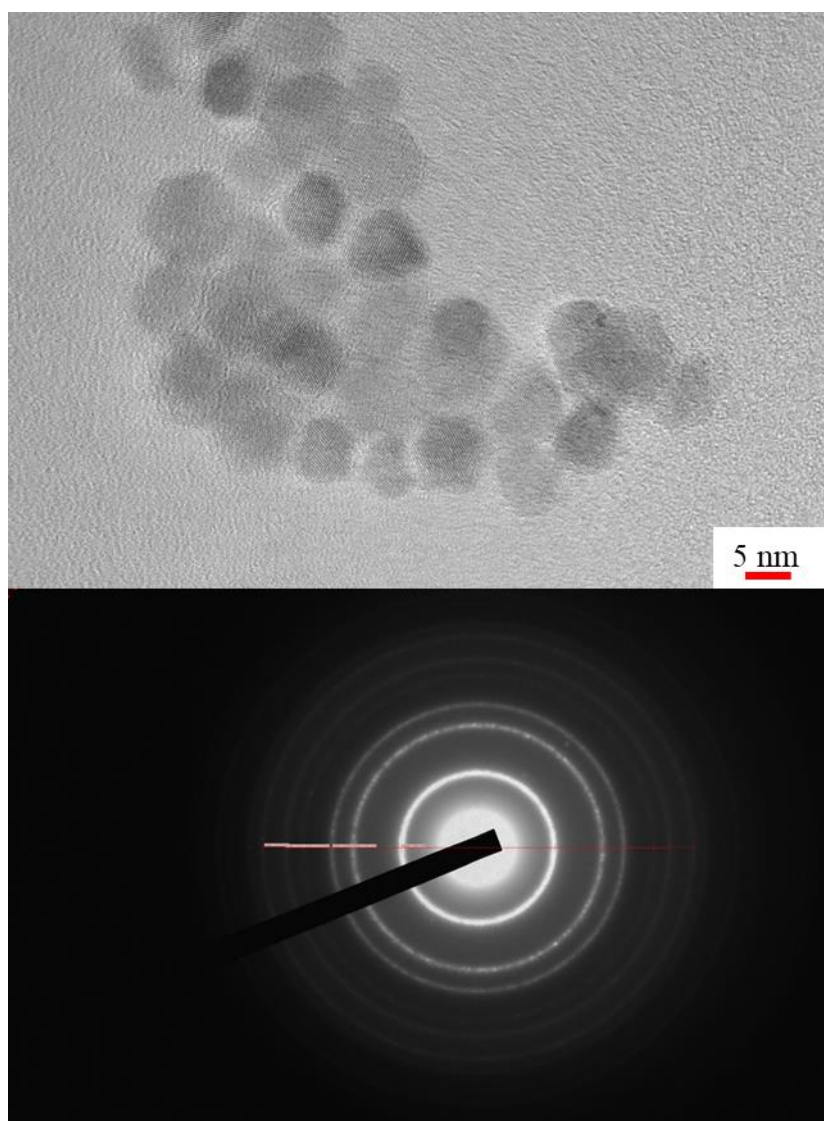


Figure 30 HRTEM and SAED image of ZnS nanoparticles at C_v of 1.8 and W_0 of 15

To summarize, the microemulsion technique enhanced by HC was successfully applied to the ZnS nanoparticles synthesis. Our experiment proved that the average size of the microemulsion can be controlled by changing the cavitation

number and the water to surfactant molar ratio. The differences in the size of microemulsion were ascribed to the turbulence intensity or the rheological properties. In the formation of the ZnS nanoparticles, the microemulsion size could significantly affect the crystallinity and particle size distribution of the resulting nanoparticles. It is found that the cavitation number and the water to surfactant molar ratio play an important role in the formation of uniform spherical shapes and narrow size distribution.



CHAPTER 5

CONCLUSIONS AND RECOMMENDATIONS

This chapter provides a key summary of this study. There are two main parts to be investigated in this work, including (i). preparation of microemulsion by hydrodynamic cavitation and (ii) synthesis of ZnS nanoparticles. However, other influential factors were also examined. The effects of cavitation number and water to surfactant molar ratio on characteristics of microemulsion and their consequent influence on the resultant ZnS are discussed. Lastly, some useful suggestions obtained during the study are provided for guiding a further investigation.

5.1 Conclusions

5.1.1 Preparation of microemulsion by hydrodynamic cavitation

In this study, synthesis of ZnS nanoparticles with variable size distribution could be achieved by microemulsion stimulated by hydrodynamic cavitation. Hydrodynamic cavitation is an effective way to the preparation of water in oil microemulsion. Multi-nozzles could be employed for generating turbulence with high intensity. The result suggested that microemulsion has been successfully prepared with small and controllable size with narrow size distribution by varying parameters. number of passages, cavitation number and water to surfactant molar ratio were found to exhibit significant effect of properties and size distribution of microemulsion.

Number of passages is a parameter corresponding to energy dissipation in the system. Increasing number of passages is related to prolongation of circulation time, therefore energy dissipation in the system was enhanced and microemulsion was fragmented into smaller size. For instance, the reduction in average size of ZnSO₄ microemulsion from 232.9 to 132.2 nm could be achieved together with an increased number of passages from 300 to 1,500 passages, However, after 1,500 passages the size remained almost constant. Moreover, with larger number of passages, the mixing of immiscible phases was enhanced, leading to the reduction of droplet size of microemulsion. Therefore, size distribution of both ZnSO₄ and Na₂S microemulsions became narrower and shifted towards smaller diameters.

The efficiency of HC was found to be dependent on cavitation number. The cavitation number was varied by changing the velocity of microemulsion pass through a multi-nozzle. Average size of ZnSO₄ and Na₂S microemulsion at 1,500 passages were decreased from 220.9 to 132.5 nm and 203.1 to 156.3 nm when C_v was decreased from 7.1 to 1.8. In addition, size distribution also became narrower and shifted towards smaller diameters. The behavior of microemulsion leading to different size distribution at various C_v was investigated using modelling by computational fluid dynamics. As observed by velocity and turbulence kinetic energy contours, the turbulence kinetic energy at multi-nozzle of C_v of 1.8 was the highest, therefore turbulence intensity increased and provide more shearing action which cause breakage in microemulsion. Consequently, microemulsion droplets as high C_v were fragmented, resulting in smaller average size and narrow size distribution.

Water to surfactant molar ratio (W_0) plays an important role in size distribution of microemulsion, as it could significantly changes rheological properties of the mixture. Based on experimental results, density, viscosity, and surface tension exhibited distinct increase at higher W_0 . it could be explained by the polarity inside water molecules which leads to the improvement of fluidity. There were several simultaneous events occurred, including in a decrease in Re and requirement of higher energy for microemulsion formation, which caused larger size of microemulsion when increasing W_0 . Therefore, the W_0 increases from 7 to 15 of 1,500 passages, the average size of ZnSO₄ and Na₂S microemulsion increases from 132.2 to 173.5 nm and from 156.3 to 177.1 nm, respectively.

Based on the investigation of the above influential factors, it is suggested that microemulsion could be prepared with controlled size and properties which could contribute to the formation of ZnS nanoparticles in confined volume of reverse micelles. Accordingly, hydrodynamic cavitation is an effective and promising method for microemulsion preparation.

5.1.2 ZnS synthesis by microemulsion method enhance by hydrodynamic cavitation

The synthesis of ZnS by microemulsion enhanced by HC is a bottom-up approach. The chemical reaction between ZnSO₄ and Na₂S took place inside reverse

micelles. then, ZnSO_4 and Na_2S microemulsion were interchanged. After that, the nucleation and growth of ZnS occurred and ZnS nanoparticles were formed. The obtained ZnS nanoparticles were spherical shape as observed in HRTEM image.

The change in average size and size distribution of resultant ZnS nanoparticles is related to the difference in microemulsion size. Therefore, varying W_0 and C_v could affect microemulsion and subsequently influence ZnS. As shown in experimental results, As shown in experimental results, increasing W_0 from 7 to 15 at C_v of 1.8 could lead to a slight increase in average size from 4.6 to 6.1 nm and size distribution became broader. However, a distinct increase in average size from 4.6 to 21.7 nm could be obtained when C_v changed from 1.8 to 7.1 while size distribution become much broader. Both W_0 and C_v altogether exhibit impact on ZnS, however, the effects of C_v is more considerable and lower C_v would be recommended to achieve size-controlled synthesis of ZnS. In addition, the successful formation of ZnS nanoparticles was also confirmed by XRD analysis. Three diffraction peaks at (111), (220) and (311) reveal the presence of cubic phase structure. Moreover, crystalline size calculated from XRD pattern is also in agreement with TEM analysis, as crystalline size increase from 4.4 to 5.1 nm with an increase in W_0 from 7 to 15.

In summary, ZnS nanoparticles with controllable size could be obtained by microemulsion enhanced by hydrodynamic cavitation as proposed in this work. Therefore, ZnS nanoparticles with small size and narrow size distribution can be considered as promising materials for various application such as electroluminescent exploration.

5.2 Recommendations

Cyclohexane is a highly flammable liquid with a petroleum-like odor and it could cause skin irritation, drowsiness or dizziness. Therefore, replacement for cyclohexane by using other alternative chemicals is recommended. The recovery and recycling of the initial substances including cyclohexane, Triton X-100 and n-hexanol should be evaluated to reduce production costs. Preparation of microemulsion should be conducted by varying cavitation number to achieve similar size distribution and the average size of ZnSO_4 and Na_2S droplets. With a controlled size of both microemulsion, ZnS nanoparticles could be obtained with better uniformity. Furthermore, the potential of applying this synthesis method in a continuous process for large-scale production should be investigated.



REFERENCES

1. Li, Y., X. He, and M. Cao, *Micro-emulsion-assisted synthesis of ZnS nanospheres and their photocatalytic activity*. Materials Research Bulletin, 2008. **43**(11): p. 3100-3110.
2. Ahmed, M., *Chapter 16 - Nanomaterial synthesis*, in *Polymer Science and Nanotechnology*, R. Narain, Editor. 2020, Elsevier. p. 361-399.
3. Malik, M.A., M.Y. Wani, and M.A. Hashim, *Microemulsion method: A novel route to synthesize organic and inorganic nanomaterials*. Arabian Journal of Chemistry, 2012. **5**(4): p. 397-417.
4. Malik, M.A., M.Y. Wani, and M.A. Hashim, *Microemulsion method: A novel route to synthesize organic and inorganic nanomaterials: 1st Nano Update*. Arabian Journal of Chemistry, 2012. **5**(4): p. 397-417.
5. Manjunatha, C., R. Hari Krishna, and S. Ashoka, *Chapter 2 - Green synthesis of inorganic nanoparticles using microemulsion methods*, in *Green Sustainable Process for Chemical and Environmental Engineering and Science*, Inamuddin, et al., Editors. 2021, Elsevier. p. 41-67.
6. Zhang, Z., et al., *Hydrodynamic cavitation as an efficient method for the formation of sub-100nm O/W emulsions with high stability*. Chinese Journal of Chemical Engineering, 2016. **24**(10): p. 1477-1480.
7. Thi Phan, K.K., et al., *Nanobubbles: Fundamental characteristics and applications in food processing*. Trends in Food Science & Technology, 2020. **95**: p. 118-130.
8. Carpenter, J., S. George, and V.K. Saharan, *Low pressure hydrodynamic cavitating device for producing highly stable oil in water emulsion: Effect of geometry and cavitation number*. Chemical Engineering and Processing: Process Intensification, 2017. **116**: p. 97-104.
9. Xiong, Z., et al., *Preparation of fluidized catalytic cracking slurry oil-in-water emulsion as anti-collapse agent for drilling fluids*. Petroleum, 2016. **2**(4): p. 361-368.
10. Azevedo, A., et al., *Aqueous dispersions of nanobubbles: Generation, properties and features*. Minerals Engineering, 2016. **94**: p. 29-37.

11. Jovanović, D.J., et al., *Synthesis and characterization of shaped ZnS nanocrystals in water in oil microemulsions*. Materials Letters, 2007. **61**(22): p. 4396-4399.
12. Dumbrava, A., et al., *The influence of Triton X-100 surfactant on the morphology and properties of zinc sulfide nanoparticles for applications in azo dyes degradation*. Materials Chemistry and Physics, 2017. **193**: p. 316-328.
13. Charinpanitkul, T., et al., *Effects of cosurfactant on ZnS nanoparticle synthesis in microemulsion*. Science and Technology of Advanced Materials, 2005. **6**(3-4): p. 266-271.
14. Fang, X., et al., *Inorganic semiconductor nanostructures and their field-emission applications*. Materials Chemistry, 2008. **18**(5): p. 509-522.
15. Khaire, R.A. and P.R. Gogate, *Application of hydrodynamic cavitation in food processing*, in *Design and Optimization of Innovative Food Processing Techniques Assisted by Ultrasound*. 2021. p. 317-342.
16. Gogate P.R., P.A.B., *Cavitation Generation and Usage Without Ultrasound: Hydrodynamic Cavitation*. Theoretical and Experimental Sonochemistry Involving Inorganic Systems, 2010: p. 69-106.
17. Meneguzzo, F., L. Albanese, and F. Zabini, *Hydrodynamic Cavitation in Beer and Other Beverage Processing*, in *Innovative Food Processing Technologies*. 2021. p. 369-394.
18. Carpenter, J., et al., *Hydrodynamic cavitation: an emerging technology for the intensification of various chemical and physical processes in a chemical process industry*. Reviews in Chemical Engineering, 2017. **33**(5).
19. Schlender, M., A. Spengler, and H.P. Schuchmann, *High-pressure emulsion formation in cylindrical coaxial orifices: Influence of cavitation induced pattern on oil drop size*. International Journal of Multiphase Flow, 2015. **74**: p. 84-95.
20. Wamankar, A.K. and S. Murugan, *Experimental investigation of carbon black–water–diesel emulsion in a stationary DI diesel engine*. Fuel Processing Technology, 2014. **125**: p. 258-266.
21. Ochowiak, M., et al., *Formation of oil/water emulsions inside the pressure-swirl atomizer*. Chemical Engineering and Processing: Process Intensification, 2017.

- 116:** p. 105-113.
22. McClements, D.J. and S.M. Jafari, *General Aspects of Nanoemulsions and Their Formulation*, in *Nanoemulsions*. 2018. p. 3-20.
 23. Vaidya, S. and A.K. Ganguli, *Microemulsion Methods for Synthesis of Nanostructured Materials*, in *Comprehensive Nanoscience and Nanotechnology*. 2019. p. 1-12.
 24. Fang, X., et al., *ZnS nanostructures: From synthesis to applications*. Progress in Materials Science, 2011. **56**(2): p. 175-287.
 25. Labiadh, H. and S. Hidouri, *ZnS quantum dots and their derivatives: Overview on identity, synthesis and challenge into surface modifications for restricted applications*. Journal of King Saud University - Science, 2017. **29**(4): p. 444-450.
 26. Fang, X., et al., *ZnO and ZnS Nanostructures: Ultraviolet-Light Emitters, Lasers, and Sensors*. Solid State and Materials Sciences, 2009. **34**(3-4): p. 190-223.
 27. Wang, Z., et al., *Application of Zero-Dimensional Nanomaterials in Biosensing*. Front Chem, 2020. **8**: p. 320.
 28. Moore, D.W., Z.L., *Growth of anisotropic one-dimensional ZnS nanostructures*. Materials Chemistry, 2006. **16**: p. 3898-3905.
 29. Ma, X., J. Song, and Z. Yu, *The light emission properties of ZnS:Mn nanoparticles*. Thin Solid Films, 2011. **519**(15): p. 5043-5045.
 30. Entezari, M.H. and N. Ghows, *Micro-emulsion under ultrasound facilitates the fast synthesis of quantum dots of CdS at low temperature*. Ultrason Sonochem, 2011. **18**(1): p. 127-34.
 31. Jangir, N., P. Diwedi, and S. Ghosh, *Design of a hydrodynamic cavitating reactor*. Chemical Engineering and Processing: Process Intensification, 2017. **122**: p. 128-142.
 32. Kiekbusch, T., et al., *Calculation of the combined torsional mesh stiffness of spur gears with two-and three-dimensional parametrical FE models*. Strojniški vestnik-Journal of Mechanical Engineering, 2011. **57**(11): p. 810-818.
 33. Zhang, Y., et al., *Cavitation optimization of single-orifice plate using CFD*

- method and neighborhood cultivation genetic algorithm.* Nuclear Engineering and Technology, 2021.
34. Saha, J. and J. Podder, *Crystallization Of Zinc Sulphate Single Crystals And Its Structural, Thermal And Optical Characterization.* Journal of Bangladesh Academy of Sciences, 2011. **35**: p. 203-210.
 35. Hwang, B.-H., et al., *Structural and optical properties of solvothermally synthesized ZnS nano-materials using Na₂S·9H₂O and ZnSO₄·7H₂O precursors.* Ceramics International, 2016. **42**(10): p. 11700-11708.
 36. Murcia, D.C.F., et al., *Determination of Zinc Sulfide Solubility to High Temperatures.* Journal of Solution Chemistry, 2017. **46**(9): p. 1805-1817.
 37. Zhu, Q., et al., *Review on the Stability Mechanism and Application of Water-in-Oil Emulsions Encapsulating Various Additives.* Compr Rev Food Sci Food Saf, 2019. **18**(6): p. 1660-1675.
 38. Faris, D., N.J. Hadi, and S.A. Habeeb, *Effect of rheological properties of (Poly vinyl alcohol/Dextrin/Naproxen) emulsion on the performance of drug encapsulated nanofibers.* Materials Today: Proceedings, 2021. **42**: p. 2725-2732.
 39. Das, S., A.P. Bhat, and P.R. Gogate, *Degradation of dyes using hydrodynamic cavitation: Process overview and cost estimation.* Journal of Water Process Engineering, 2021. **42**: p. 102126.
 40. Fathi Roudsari, S., et al., *CFD modeling of the mixing of water in oil emulsions.* Computers & Chemical Engineering, 2012. **45**: p. 124-136.
 41. Pukkella, A.K., et al., *Improved mixing of solid suspensions in stirred tanks with interface baffles: CFD simulation and experimental validation.* Chemical Engineering Journal, 2019. **358**: p. 621-633.
 42. Sartomo, A., et al., *Recent progress on mixing technology for water-emulsion fuel: A review.* Energy Conversion and Management, 2020. **213**.
 43. Tang, S.Y., P. Shridharan, and M. Sivakumar, *Impact of process parameters in the generation of novel aspirin nanoemulsions--comparative studies between ultrasound cavitation and microfluidizer.* Ultrason Sonochem, 2013. **20**(1): p. 485-97.
 44. Sarkar, J., et al., *CFD of mixing of multi-phase flow in a bioreactor using*

- population balance model*. Biotechnol Prog, 2016. **32**(3): p. 613-28.
45. Wang, J., et al., *Synthesis and size control via variation of temperature of ZnSe:Fe nanocrystals in a microemulsion assisted hydrothermal system*. Materials Chemistry and Physics, 2022. **276**.
 46. Farah, M.A., et al., *Viscosity of water-in-oil emulsions: Variation with temperature and water volume fraction*. Journal of Petroleum Science and Engineering, 2005. **48**(3-4): p. 169-184.
 47. Tatar, B.C., G. Sumnu, and S. Sahin, *Rheology of Emulsions*. Advances in Food Rheology and Its Applications, 2017: p. 437-457.
 48. Azevedo, A., H. Oliveira, and J. Rubio, *Bulk nanobubbles in the mineral and environmental areas: Updating research and applications*. Adv Colloid Interface Sci, 2019. **271**: p. 101992.
 49. Mandato, S., et al., *Liquids' atomization with two different nozzles: Modeling of the effects of some processing and formulation conditions by dimensional analysis*. Powder Technology, 2012. **224**: p. 323-330.
 50. Ithnin, A.M., et al., *Combustion performance and emission analysis of diesel engine fuelled with water-in-diesel emulsion fuel made from low-grade diesel fuel*. Energy Conversion and Management, 2015. **90**: p. 375-382.
 51. Charinpanitkul, T., et al., *Effects of cosurfactant on ZnS nanoparticle synthesis in microemulsion*. Science and Technology of Advanced Materials, 2005. **6**(3): p. 266-271.
 52. Eastoe, J., M.J. Hollamby, and L. Hudson, *Recent advances in nanoparticle synthesis with reversed micelles*. Advances in Colloid and Interface Science, 2006. **128-130**: p. 5-15.
 53. Rauscher, F., P. Veit, and K. Sundmacher, *Analysis of a technical-grade w/o-microemulsion and its application for the precipitation of calcium carbonate nanoparticles*. Colloids and Surfaces A: Physicochemical and Engineering Aspects, 2005. **254**(1): p. 183-191.
 54. Rajoriya, S., S. Bargole, and V.K. Saharan, *Degradation of a cationic dye (Rhodamine 6G) using hydrodynamic cavitation coupled with other oxidative agents: Reaction mechanism and pathway*. Ultrasonics Sonochemistry, 2017. **34**:

- p. 183-194.
55. Latsuzbaia, R., E. Negro, and G. Koper, *Bicontinuous microemulsions for high yield, wet synthesis of ultrafine nanoparticles: a general approach*. Faraday Discuss, 2015. **181**: p. 37-48.
 56. Pileni, M.P., *Mesostructured fluids in oil-rich regions: Structural and templating approaches*. Langmuir, 2001. **17**(24): p. 7476-7486.
 57. Barman, B. and K. Chandra Sarma, *Low temperature chemical synthesis of ZnS, Mn doped ZnS nanosized particles: Their structural, morphological and photophysical properties*. Solid State Sciences, 2020. **109**: p. 106404-106404.
 58. Khiew, P.S., et al., *Preparation and characterization of ZnS nanoparticles synthesized from chitosan laurate micellar solution*. Materials Letters, 2005. **59**(8-9): p. 989-993.
 59. Ranjan, R., et al., *Controlling the Size, Morphology, and Aspect Ratio of Nanostructures Using Reverse Micelles: A Case Study of Copper Oxalate Monohydrate*. Langmuir, 2009. **25**(11): p. 6469-6475.
 60. Borah, J.P., J. Barman, and K. Sarma, *Structural and optical properties of ZnS nanoparticles*. Chalcogenide Lett, 2008. **5**(9): p. 201-208.
 61. Liu, J., et al., *Synthesis of ZnS nanoparticles via hydrothermal process assisted by microemulsion technique*. Journal of Alloys and Compounds, 2009. **486**(1-2): p. L40-L43.
 62. Raj, D.V., C.J. Raj, and S.J. Das, *Synthesis and optical properties of cerium doped zinc sulfide nano particles*. Superlattices and Microstructures, 2015. **85**: p. 274-281.



APPENDIX

จุฬาลงกรณ์มหาวิทยาลัย
CHULALONGKORN UNIVERSITY

APPENDIX A CALCULATION

Calculation of cavitation number

$$C_v = \frac{P_2 - P_v}{\frac{1}{2} \rho v^2}$$

fully recovered downstream pressure (P_2) = 102,171.77 (N m⁻²)

vapor pressure of the aqueous solution (P_v) = 2,300 (N m⁻²)

density of the aqueous solution (ρ) = 997 (kg m⁻³)

superficial velocity of the circulated microemulsion (v) = 10.62 (m s⁻¹)

$$C_v = \frac{102,171.77 - 2,300}{\frac{1}{2}(997)(10.62^2)} = 1.8$$

Table A1 Flow rate, velocity, and cavitation number

Q (L/min)	Velocity (m/s)	C_v
12.0	10.62	1.8
9.0	7.96	3.2
6.0	5.31	7.1

Calculation of number of passages

$$\text{Number of passages} = \frac{\text{Volumetric flow rate}}{\text{Total volume of emulsion}} \times \text{circulation time}$$

$$300 = \frac{12 \text{ L/min}}{0.7 \text{ L}} \times \text{circulation time}$$

$$\text{circulation time at 300 passages} = 17.35 \text{ min}$$

Calculation of water to surfactant molar ratio

Studied the influence of the molar ratio of water to surfactant (W_0) at 7, 11, and 15

$$W_0 = \frac{[H_2O]}{[Surfactant]}$$

M_w of water = 18.0 g/mol

M_w of Triton X-100 = 625.1 g/mol

$$7 = \frac{[g \text{ of water}/18]}{[147.7 \text{ g}/625]}$$

$$g \text{ of water} = 29.7 \text{ g}$$

Table A2 Amount of reactant

W_0	amount of reactant (ml)	Cyclohexane (ml)	Triton X-100 (ml)	n-hexanol (ml)
7	29.7	500	138	26
11	46.7	500	138	26
15	63.7	500	138	26

Calculation of energy dissipation in system

$$E = P \times V \times t$$

pressure drop across a multi nozzle (P) = 81,373.9 (N m⁻²)

volumetric flow rate (V) = 8.33 × 10⁻⁶ (m³ s⁻¹)

circulation time (t) at 300 passages = 1,041 (s)

$$E = 81,373.9 \times 8.33 \times 10^{-6} \times 1,041 = 706 \text{ J}$$

Table B2 Average size, standard deviation size distribution of ZnSO₄ and Na₂S microemulsion $C_p = 1.8$ $W_0=11$

Size (nm)	ZnSO ₄					Na ₂ S				
	Intensity (%)					Intensity (%)				
	300	600	900	1,200	1,500	300	600	900	1,200	1,500
D _{avg}	241.3	179.6	173.9	139.1	138.5	325.7	234.3	205.6	178.4	162.0
SD	1.2	1.2	1.2	1.2	1.1	1.7	1.3	1.2	1.2	1.2
10.1	0.0	0.0	0.0	0.0	0.0	0.0	0.0	0.0	0.0	0.0
11.7	0.0	0.0	0.0	0.0	0.0	0.0	0.0	0.0	0.0	0.0
13.54	0.0	0.0	0.0	0.0	0.0	0.0	0.0	0.0	0.0	0.0
15.69	0.0	0.0	0.0	0.0	0.0	0.0	0.0	0.0	0.0	0.0
18.17	0.0	0.0	0.0	0.0	0.0	0.0	0.0	0.0	0.0	0.0
21.04	0.0	0.0	0.0	0.0	0.0	0.0	0.0	0.0	0.0	0.0
24.36	0.0	0.0	0.0	0.0	0.0	0.0	0.0	0.0	0.0	0.0
28.21	0.0	0.0	0.0	0.0	0.0	0.0	0.0	0.0	0.0	0.0
32.67	0.0	0.0	0.0	0.0	0.0	0.0	0.0	0.0	0.0	0.0
37.84	0.0	0.0	0.0	0.0	0.0	0.0	0.0	0.0	0.0	0.0
43.82	0.0	0.0	0.0	0.0	0.0	0.0	0.0	0.0	0.0	0.0
50.75	0.0	0.0	0.0	0.0	0.0	0.0	0.0	0.0	0.0	0.0
58.77	0.0	0.0	0.0	0.0	0.0	0.0	0.0	0.0	0.0	0.0
68.06	0.0	0.0	0.0	0.0	0.0	0.0	0.0	0.0	0.0	0.0
78.82	0.0	0.0	0.0	0.0	0.0	0.0	0.0	0.0	0.0	0.0
91.28	0.0	0.0	0.0	0.0	2.2	0.0	0.0	0.0	0.0	0.0
105.7	0.0	0.0	0.0	8.5	10.3	0.0	0.0	0.0	0.0	0.0
122.4	0.0	0.0	1.9	28.2	25.9	0.0	0.0	0.0	5.1	11.3
141.8	0.0	14.2	19.8	35.7	32.6	0.2	2.9	4.1	17.0	24.7
164.2	0.2	32.5	34.3	23.0	22.3	2.4	10.7	16.9	27.0	31.6
190.1	15.0	34.1	29.7	4.6	6.7	8.7	18.0	29.1	26.3	23.6
220.2	31.4	17.8	12.5	0.0	0.0	15.3	21.8	28.0	16.3	8.8
255	32.6	1.4	1.9	0.0	0.0	18.1	20.0	16.2	6.9	0.0
295.3	18.1	0.0	0.0	0.0	0.0	15.9	14.4	5.9	1.3	0.0
342	2.7	0.0	0.0	0.0	0.0	10.7	8.8	0.0	0.0	0.0
396.1	0.0	0.0	0.0	0.0	0.0	6.4	3.2	0.0	0.0	0.0
458.7	0.0	0.0	0.0	0.0	0.0	5.4	0.2	0.0	0.0	0.0
531.2	0.0	0.0	0.0	0.0	0.0	5.2	0.0	0.0	0.0	0.0
615.1	0.0	0.0	0.0	0.0	0.0	4.4	0.0	0.0	0.0	0.0
712.4	0.0	0.0	0.0	0.0	0.0	3.2	0.0	0.0	0.0	0.0
825	0.0	0.0	0.0	0.0	0.0	1.9	0.0	0.0	0.0	0.0
955.4	0.0	0.0	0.0	0.0	0.0	0.8	0.0	0.0	0.0	0.0

APPENDIX C

YIELD OF SYNTHESIZED ZNS NANOPARTICLES

From equation 13, mole of $ZnSO_4$ is depleted consumption with assuming complete reaction. Calculation amount of ZnS nanoparticles product was shown below.

$$\text{Mole of } ZnSO_4 = \text{Mole of } ZnS$$

$$W_0 = 7$$

$$\frac{MV}{1000} = \frac{g \text{ of } ZnS}{M_w}$$

$$0.1 \frac{\text{mole}}{L} \times 27.77 \text{ ml} \times \frac{1 L}{1000 \text{ ml}} = \frac{\text{amount of } ZnS}{97.47}$$

$$\text{amount of } ZnS = 0.29g$$

Table C1 Yield of synthesized ZnS nanoparticles

C_v	W_0	yield of synthesized product			
1.8	15	94.3	94.8	97.5	95.5±1.7
	11	91.3	93.0	94.1	92.8±1.4
	7	89.0	90.8	91.1	90.3±1.1
3.2	7	86.3	87.2	87.9	87.1±0.8
7.1	7	81.8	82.6	82.8	82.40.5

APPENDIX D
TEM IMAGES OF ZNS NANOPARTICLES

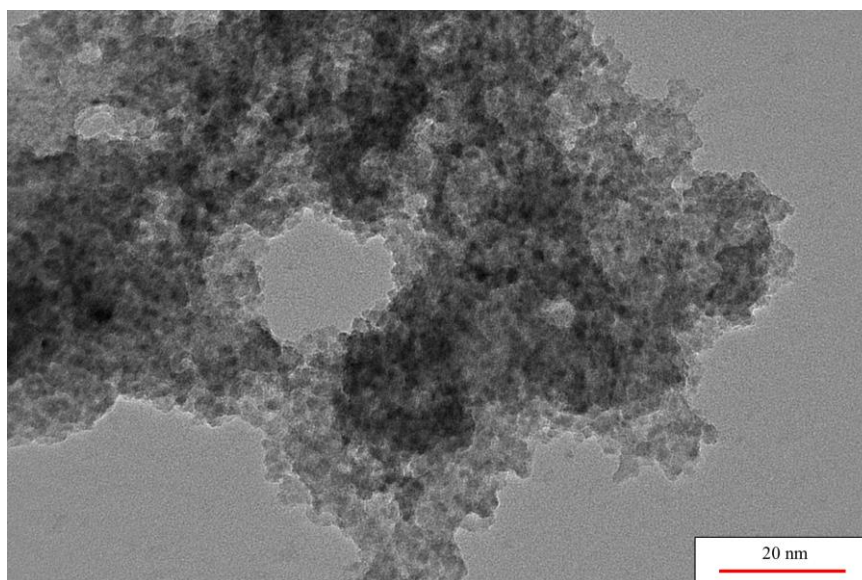


Figure D-1 TEM micrograph of ZnS nanoparticles ($C_v=1.8$, $W_0=7$)

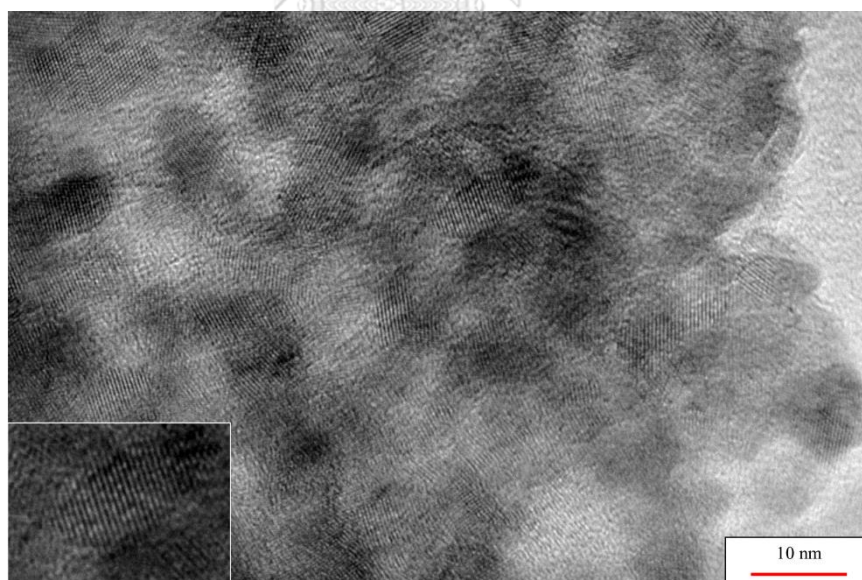


Figure D-2 TEM micrograph of ZnS nanoparticles ($C_v=1.8$, $W_0=7$)

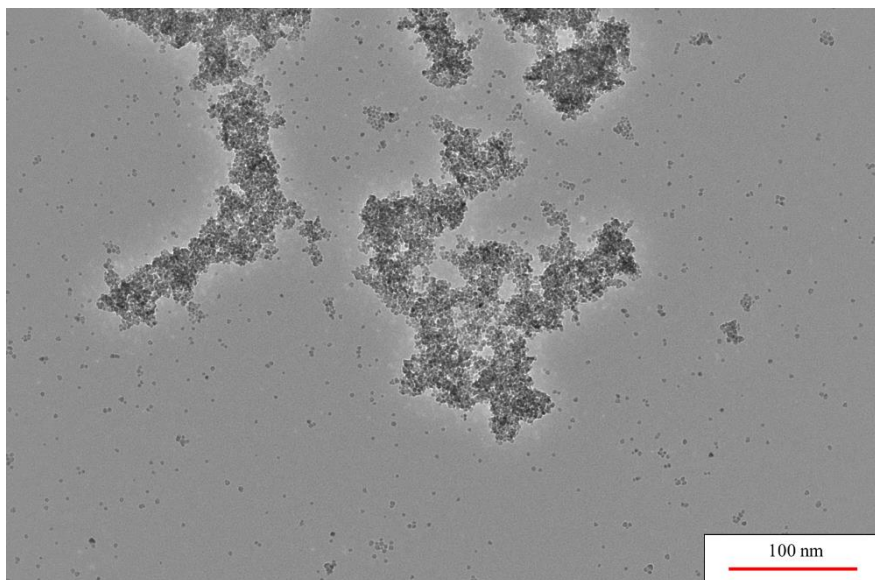


Figure D-3 TEM micrograph of ZnS nanoparticles ($C_v=1.8$, $W_0=11$)

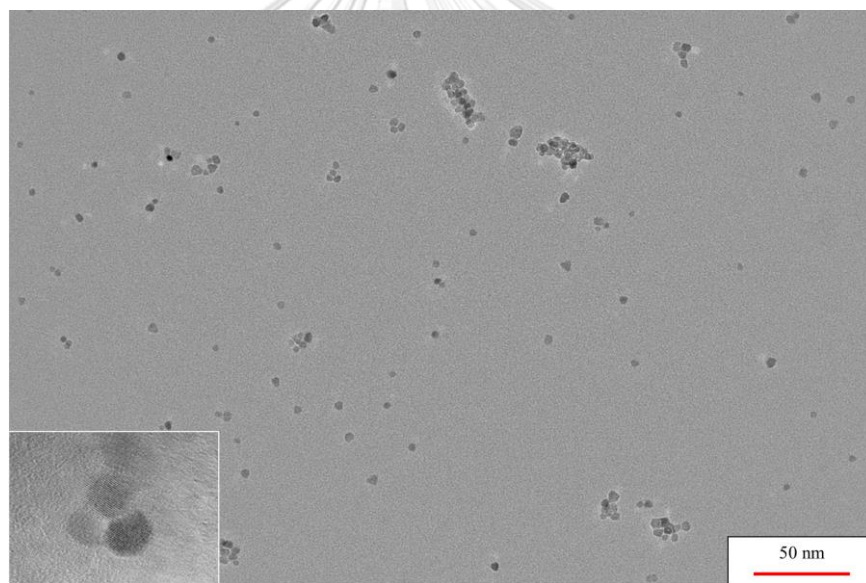


Figure D-4 TEM micrograph of ZnS nanoparticles ($C_v=1.8$, $W_0=11$)

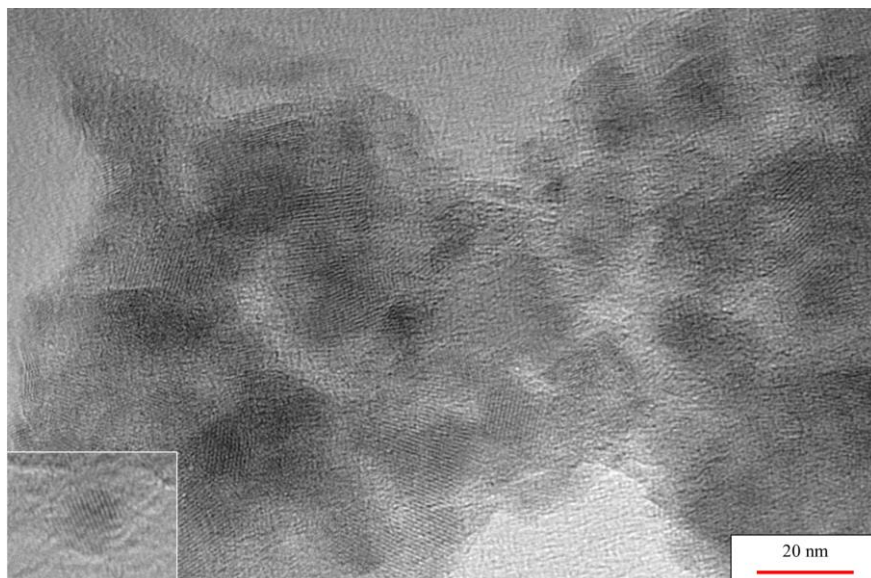


Figure D-5 TEM micrograph of ZnS nanoparticles ($C_v=1.8$, $W_0=15$)

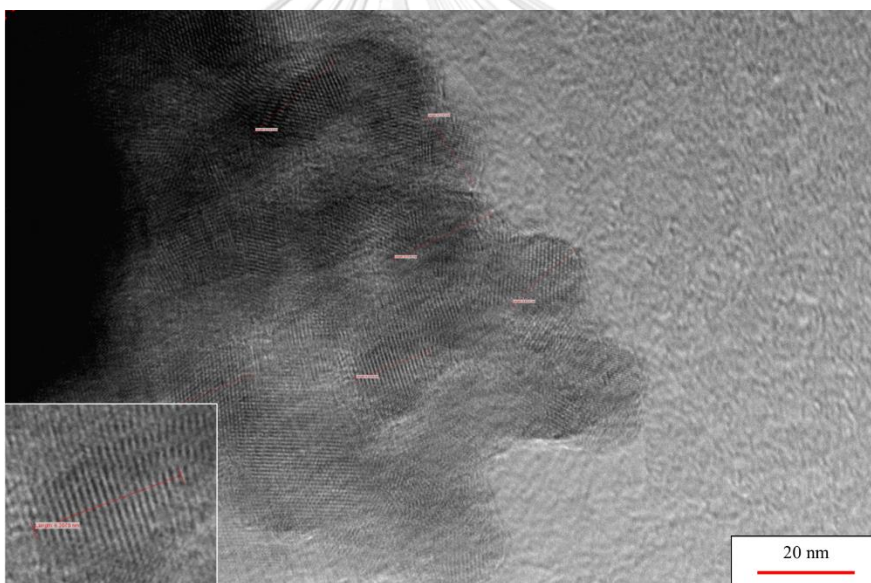


Figure D-6 TEM micrograph of ZnS nanoparticles ($C_v=3.2$, $W_0=7$)

APPENDIX E

EDX SPECTRUM OF TYPICAL ZNS NANOPARTICLES

EDX analysis is an important analytical tool to determine the composition of the sample. The result was conducted to reveal that these products are ZnS nanoparticles. The spectra reveal that only two elements Zn, S exist in pure ZnS nanoparticles. No traces of other elements were found in the spectra confirms the purity of the sample as shown in **Figure E-1**.

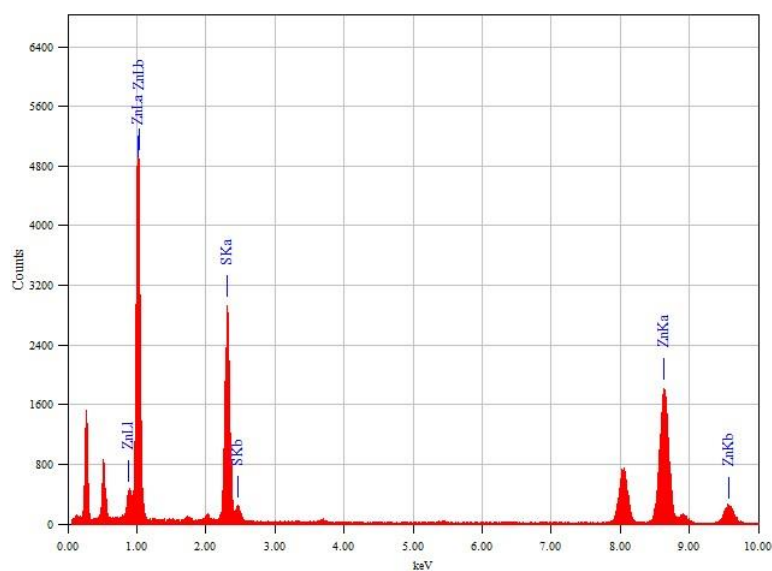


Figure D-1 EDX spectrum of ZnS nanoparticles by JEM-2100(URP)

APPENDIX F

SCHEMATIC DIAGRAM AND DIMENSION OF THE EXPERIMENTAL SETUP

The schematic diagram and dimension of the experimental setup for microemulsion preparation was shown in **Figure F-1** and **Table F-1**.

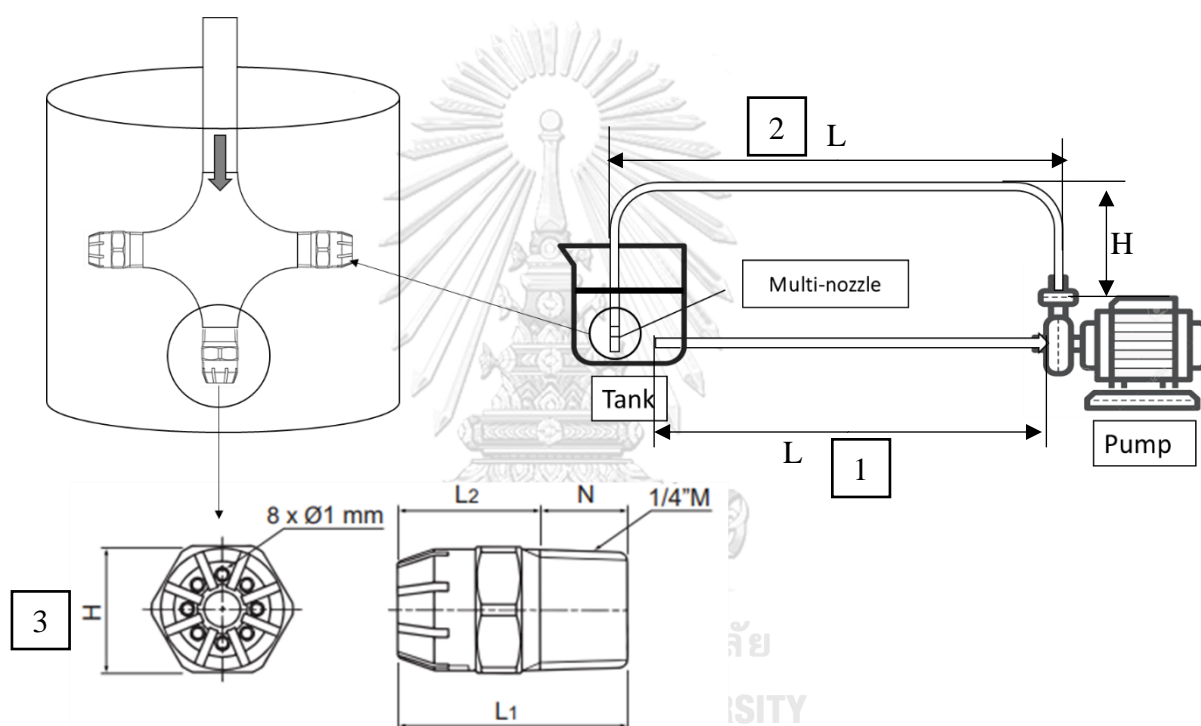


Figure F-1 schematic diagram of the experimental setup

Table F-1 Dimension and material of pipe and multi-nozzle

	Material	Dimension (mm)
1	PVC	$\text{Ø}=25.4$ and $L=200$
2	PVC	$\text{Ø}=25.4$, $L=200$ and $H=50$
3	SS 304	$\text{Ø}=1$, $L_1=25$, $L_2=15.5$, $N=9.5$ and $H=14$

VITA

NAME Nachapa Choojan

DATE OF BIRTH 25 February 1997

PLACE OF BIRTH Choburi

INSTITUTIONS ATTENDED

- Bachelor's Degree of Engineering (Chemical Engineering), King Mongkut's University of Technology North Bangkok (KMUTNB), Bangkok, Thailand, 2018.
- Studying Master's Degree of Engineering (Chemical Engineering), Chulalongkorn University, Bangkok, Thailand, since 2019.

HOME ADDRESS 137/33 Nongirun, Banbung, Choburi, 20220

PUBLICATION

- Choojan, N., Viphavakit, C., and Charinpanitkul, T. (2021) Effect of water to surfactant molar ratio on characteristics of ZnS nanoparticles synthesized by microemulsion enhanced by hydrodynamic cavitation. JCREN 2021's proceeding.
- Choojan, N., Wandaw, R., Rodruangnon, T., Laitha, K., Chantawong, T., Viphavakit, C., and Charinpanitkul, T. (2020) Investigation on size distribution and zeta potential of Ultrafine Bubbles in Water. JCREN 2020's proceeding.

AWARD RECEIVED Outstanding Oral Presentation Award in The 9th Joint Conference on Renewable Energy and Nanotechnology (JCREN 2020).